

The Production of Photons with Large Transverse Momentum

J.F. Owens

Physics Department, Florida State University

2012 CTEQ Summer School

July 30 - August 9, 2012

Lima, Peru

Outline

1. Introduction

- Why photons?

2. Theory overview

- Pointlike and Fragmentation components
- Photon isolation

3. Comparison to data

- Isolated cross sections, Inclusive cross sections

4. Theoretical improvements

- Resummation

5. Conclusions

6. Appendix: Notation, kinematics, and other useful information

Why Photons?

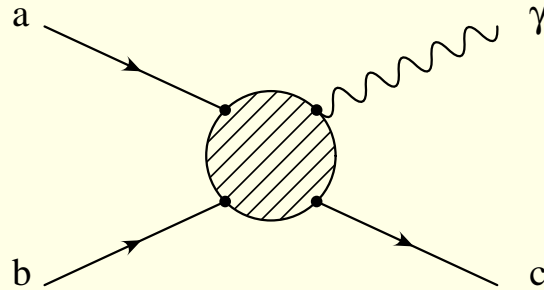
- Well understood electromagnetic interaction
- Well defined probe of strong interaction dynamics
- Classic examples
 - Deep inelastic scattering
 - Lepton pair production
 - $e^+e^- \rightarrow$ hadrons
- Direct photons, photoproduction, and two photon processes continue this history

Reasons to study photon production

- Gluon PDF is rather indirectly constrained
 - Momentum sum rule
 - Q^2 dependence of PDFs in DIS via DGLAP equations
 - Jet production at colliders via $gg \rightarrow gg$ and $gq \rightarrow gq$, but $qq \rightarrow qq$ dominates at high values of p_T
- QCD Compton process $gq \rightarrow \gamma q$ appears at lowest order only with $q\bar{q} \rightarrow \gamma g$ so looks to provide an ideal way to constrain the gluon PDF
- Intrinsic interest in seeing if QCD properly describes the photon production mechanisms - offers a new way of looking at QCD dynamics
- Photons are essential for certain search strategies at the LHC, *e.g.*, $H \rightarrow 2\gamma$, so photon production must be understood in order to control the backgrounds for such searches

Theory Overview

- Lowest Order: $\mathcal{O}(\alpha\alpha_s)$
 1. $qg \rightarrow \gamma g$ QCD Compton
 2. $q\bar{q} \rightarrow \gamma g$ annihilation
- The single photon invariant cross section is given by a convolution with the beam and target parton distribution functions



$$d\sigma(AB \rightarrow \gamma + X) = G_{a/A}(x_a, \mu_F) dx_a G_{b/B}(x_b, \mu_F) dx_b \frac{1}{2\hat{s}} \sum_{ab} \overline{|M(ab \rightarrow \gamma c)|^2} d^2 PS$$

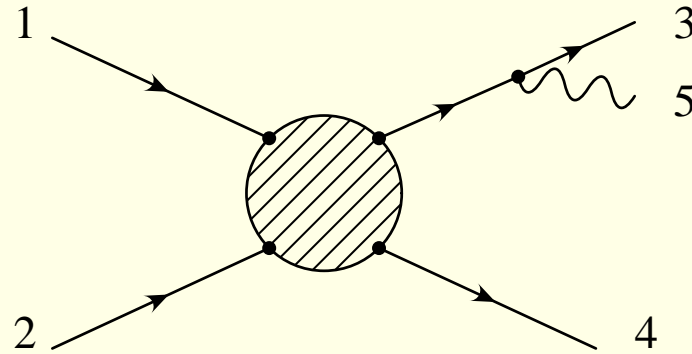
- $d^2 PS$ denotes two-body phase space and μ_F is the factorization scale

- See the appendix for more details about variables and four-vectors
- Also see the Handbook of Perturbative QCD on the CTEQ web site <http://www.cteq.org>. The appendix has additional information on how to calculate cross sections for hadronic processes starting at the parton level.

Next-to-Leading Order: $\mathcal{O}(\alpha\alpha_s^2)$

1. one-loop virtual contributions
 2. $q\bar{q} \rightarrow \gamma gg$
 3. $gq \rightarrow \gamma qg$
 4. $qq' \rightarrow \gamma qq'$ plus related subprocesses
- In the next order one sees a new configuration wherein the photon is no longer isolated. Instead, it may be radiated off a high- p_T quark produced in the hard scattering process.

- Consider the subprocess $q(1)q(2) \rightarrow q(3)q(4)\gamma(5)$
- Examine the region where $s_{35} = (p_3 - p_5)^2 \approx 0$



$$\overline{\sum} |M(qq \rightarrow qq\gamma)|^2 \approx \frac{\alpha}{2\pi} P_{\gamma q}(z) \frac{1}{s_{35}} \overline{\sum} |M(qq \rightarrow qq)|^2$$

- An internal quark line is going on-shell signalling long distance physics effects
- Gives rise to a collinear singularity
- Can factorize the singularity by introducing a *photon fragmentation function*

Photon Fragmentation

- Photon is accompanied by jet fragments on the *same* side
- Factorize the singularity and include it in the bare photon fragmentation function
- Sum large logs with modified Altarelli-Parisi equations

$$Q^2 \frac{dD_{\gamma/q}(x, Q^2)}{dQ^2} = \frac{\alpha}{2\pi} P_{\gamma q} + \frac{\alpha_s}{2\pi} [D_{\gamma/q} \otimes P_{qq} + D_{\gamma/g} \otimes P_{gq}]$$

$$Q^2 \frac{dD_{\gamma/g}(x, Q^2)}{dQ^2} = \frac{\alpha_s}{2\pi} \left[\sum_q D_{\gamma/q} \otimes P_{qg} + D_{\gamma/g} \otimes P_{gg} \right]$$

- As with hadron pdfs and fragmentation functions, can't perturbatively calculate the fragmentation functions, but the scale dependence is perturbatively calculable
- Note the $P_{\gamma q}$ splitting function - represents the pointlike coupling of the photon to the quark in $q \rightarrow \gamma q$

Fragmentation Component

- The situation has become more complex
- Expect to see two classes of events
 1. Direct (or pointlike) - no hadrons accompanying the photon
 2. Fragmentation (or bremsstrahlung) - photon is a fragment of a high- p_T jet. Part of the fragmentation function is perturbatively calculable.
- Expect (1) to dominate at high- p_T since the energy is not shared with accompanying hadrons.
- The $P_{\gamma q}$ splitting function gives rise to the leading high Q^2 behavior going as $\alpha \log(Q^2/\Lambda^2) \sim \frac{\alpha}{\alpha_s}$ (see the Appendix for a derivation)

So, to our list of contributions add those involving **photon fragmentation functions**

- $\mathcal{O}(\alpha\alpha_s) : \frac{d\sigma}{d\hat{t}}(ab \rightarrow cd) \otimes D_{\gamma/c}$
- $\mathcal{O}(\alpha\alpha_s^2) : \frac{d\sigma}{d\hat{t}}(ab \rightarrow cde) \otimes D_{\gamma/c}$

A nagging question

- The perturbative part of the photon fragmentation functions first showed up in our examples at the next to leading order in α_s , that is, one order beyond the Born term. Are they just higher order corrections then?
- Not really. When one examines solutions of the relevant evolution equations, it becomes apparent that the leading behavior of the perturbative part of the solutions goes as $\ln Q^2$. This is quite different from the usual hadronic behavior where we are used to seeing the distributions decrease at large x and slowly increase at small x . (See additional notes at the end of the lecture)
- The factor of $\ln Q^2$ effectively cancels out one factor of α_s , so that the fragmentation and direct contributions end up having similar dependences on Q^2 . We should have included these pieces even at the lowest order!

Some Comments

- Photons can be produced as fragments of jets, as is also the case for particles
- Photon production therefore involves all of the subprocesses relevant for jet or particle production
- In addition, one also has the pointlike production processes

Photon production is *more* complicated than jet production, not *less*

Next-to-leading-order Calculations

- Have to integrate over unobserved partons. There are regions of phase space where partons can become parallel to each other (collinear) or soft. Both regions are singular.
- Usually use dimensional regularization to regulate the divergences

Two types of programs exist

1. Phase space integrations done symbolically so expressions for the integrated parton-level subprocess cross sections exist. Integrations over the parton momentum fractions x_a, x_b , and z_c done numerically. This approach is suitable for the single photon inclusive cross section.
2. All integrations done via Monte Carlo
 - Phase space slicing method
 - Subtraction method

With Monte Carlo programs one can examine correlations between the photon and other partons in the final state.

Phase Space Slicing Monte Carlo

- See B. Harris and J.F. Owens hep-ph/0102128, Phys. Rev. **D65** 094032 (2002).
- Work in $n=4-2\epsilon$ dimensions using dimensional regularization
- Notation:
 - At the parton level: $p_1 + p_2 \rightarrow p_3 + p_4 + p_5$
 - Let $s_{ij} = (p_i + p_j)^2$ and $t_{ij} = (p_i - p_j)^2$
- Partition $2 \rightarrow 3$ phase space into three regions
 1. Soft: gluon energy $E_g < \delta_s \sqrt{s_{12}}/2$
 2. Collinear: s_{ij} or $|t_{ij}| < \delta_c s_{12}$
 3. Finite: everything else

- In the soft region use the soft gluon approximation to generate a simple expression for the squared matrix element which can be integrated by hand
- In the collinear region use the leading pole approximation to generate a simple expression which can be integrated by hand.
- Resulting expressions have explicit poles from soft and collinear singularities
- Factorize initial and final state mass singularities and absorb into the fragmentation and distribution functions
- Add soft and collinear integrated results to the $2 \rightarrow 2$ contributions – singularities cancel
- Generate finite region contributions in 4 dimensions using usual Monte Carlo techniques
- End result is a set of two-body weights and a set of three-body weights.
- Both are finite and both depend on the cutoffs δ_s and δ_c

Cutoff dependence cancels for sufficiently small cutoffs when the two sets of weights are added at the histogramming stage

Simple example - consider the integral of a quantity which has a pole at $x = 0$. Using dimensional regularization, one has an integral of the form

$$F = \int_0^1 dx x^{-1-\epsilon} f(x).$$

For x very near zero, approximate $f(x)$ by $f(0)$ yielding

$$F \approx f(0) \int_0^\delta dx x^{-1-\epsilon} + \int_\delta^1 dx x^{-1-\epsilon} f(x).$$

The first integral can be done analytically. The second is finite and can be evaluated with $\epsilon = 0$.

$$F \approx -\frac{f(0)}{\epsilon} + f(0) \log \delta + \int_\delta^1 dx \frac{f(x)}{x}.$$

The second integral can be done numerically. The dependence on the cutoff δ cancels for sufficiently small values of δ

Direct Photon Cross sections Inclusive versus Isolated

Inclusive cross section

- Measure the photon at some rapidity and p_T with no constraints on any of the accompanying particles
- Theoretically, one includes both the pointlike and fragmentation components
- This observable is theoretically the most straightforward to calculate

Isolated cross section

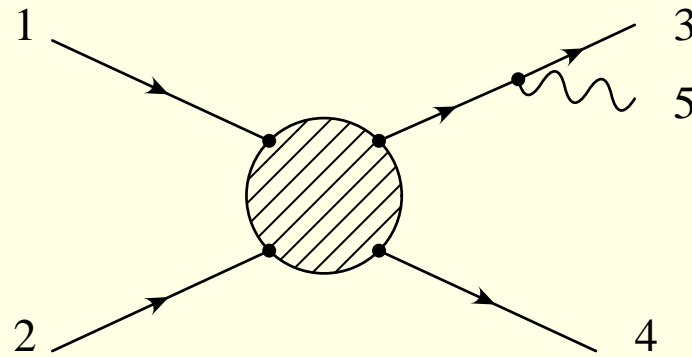
- Place restrictions on the energy of the particles that are nearby the photon in phase space
- May be part of the electromagnetic trigger used to define the photon signal
- Aim is to reduce the fragmentation contribution leaving something which is closer to what is expected for the pointlike component

Using lowest order subprocesses, the cross section can be written as

$$E \frac{d^3\sigma}{dp^3}(AB \rightarrow \gamma + X) = \sum_{abc} \int dx_a dx_b dz G_{a/A}(x_a, \mu_F) G_{b/B}(x_b, \mu_F) \\ \frac{\hat{s}}{\pi} \delta(\hat{s} + \hat{t} + \hat{u}) \left[\frac{d\sigma}{d\hat{t}}(ab \rightarrow \gamma + d) \delta(1 - z) + \frac{d\sigma}{d\hat{t}}(ab \rightarrow cd) D_{\gamma/c}(z, \mu_f) \right]$$

- The pointlike and fragmentation pieces are clearly separated since the latter involves the fragmentation functions
- At lowest order, the ratio of the pointlike and fragmentation contributions is well defined
- This is no longer true once one goes to higher orders
- Part of the fragmentation function is perturbatively calculable from the $q \rightarrow \gamma q$ vertex

For example, consider the subprocess $qq' \rightarrow \gamma qq'$ discussed previously



$$\overline{\sum} |M(qq \rightarrow qq\gamma)|^2 \approx \frac{\alpha}{2\pi} P_{\gamma q}(z) \frac{1}{s_{35}} \overline{\sum} |M(qq \rightarrow qq)|^2$$

- The collinear singularity resulting when the photon and quark are collinear must be factorized and absorbed into the bare fragmentation function
- This introduces a factorization scale μ_f
 - The fragmentation function depends on μ_f and the full dependence can be calculated using the DGLAP equations (see the Appendix)
 - The remaining hard scattering contribution also has a dependence on μ_f

- One sees that this calculable perturbative subprocess contributes to the fragmentation process - the photon is accompanied by associated partons nearby
- There is no longer a clean separation between the two contributions
- Although one can't uniquely separate the two components, it is possible to reduce the fragmentation contribution using an **isolation cut**
- Isolation cuts may be imposed
 - As part of the experimental trigger used to define a photon
 - Because one might want to reduce the influence of the fragmentation component (more on this later)
- All isolation cuts seek to remove a portion of the signal where hadronic fragments occur in close association with the photon

Specific Example - cone algorithm

- Require that there be less than 1 GeV of hadronic transverse energy in a cone of radius

$$\mathcal{R} = \sqrt{(\Delta\eta)^2 + (\Delta\phi)^2} < 0.4$$

about the direction of the photon.

Theoretical modeling (phase space slicing method)

- Must treat the two- and three-body contributions separately
- For the $2 \rightarrow 3$ pointlike subprocesses, one can explicitly enforce the isolation condition on an event-by-event basis in the Monte Carlo at the parton level.

- For the two-body fragmentation component there is no dependence on \mathcal{R} since the fragmentation functions are inclusive quantities.
 - Work in the collinear approximation (all emitted partons or photons are collinear with the parent parton)
 - parent parton transverse momentum is p_{Tpart}
 - photon transverse momentum is $p_{T\gamma} = zp_{Tpart}$
 - hadronic E_T is $(1 - z)p_{Tpart} = (1 - z)p_{t\gamma}/z$.
- Requiring that the hadronic E_T is less than E_{Tcut} results in

$$z > \frac{1}{1 + E_{Tcut}/p_{T\gamma}}.$$

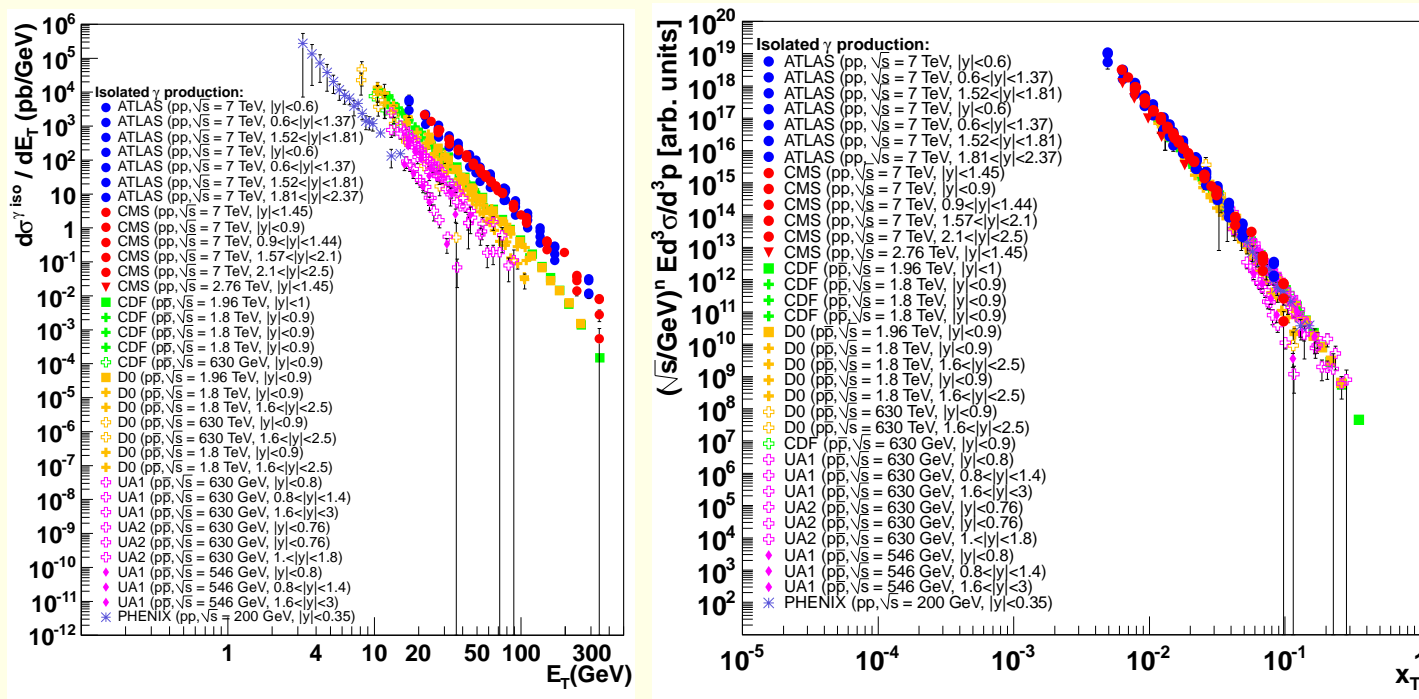
- One can also enforce a similar isolation condition on the $2 \rightarrow 3$ fragmentation component

Comparison to data

First, examine the isolated cross section data since most collider experiments measure isolated cross sections.

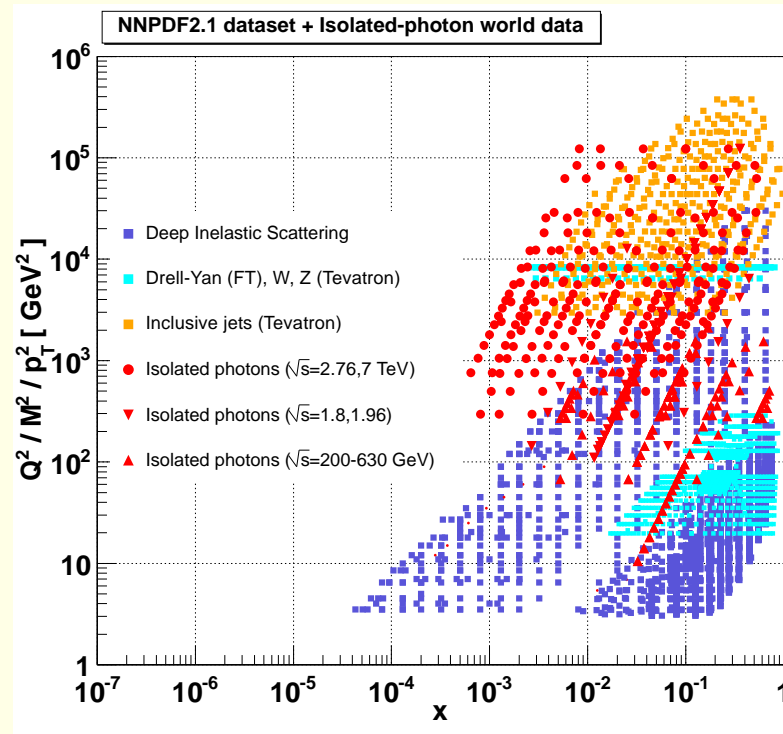
- Results are from an analysis by D. d'Enterria and J. Rojo, arXiv:1202.1762[hep-ph]
- Use NNPDF2.1 PDFs and study the isolated photon cross section
- Data are self consistent
- Theory gives good agreement over a wide kinematic range

Data Summary



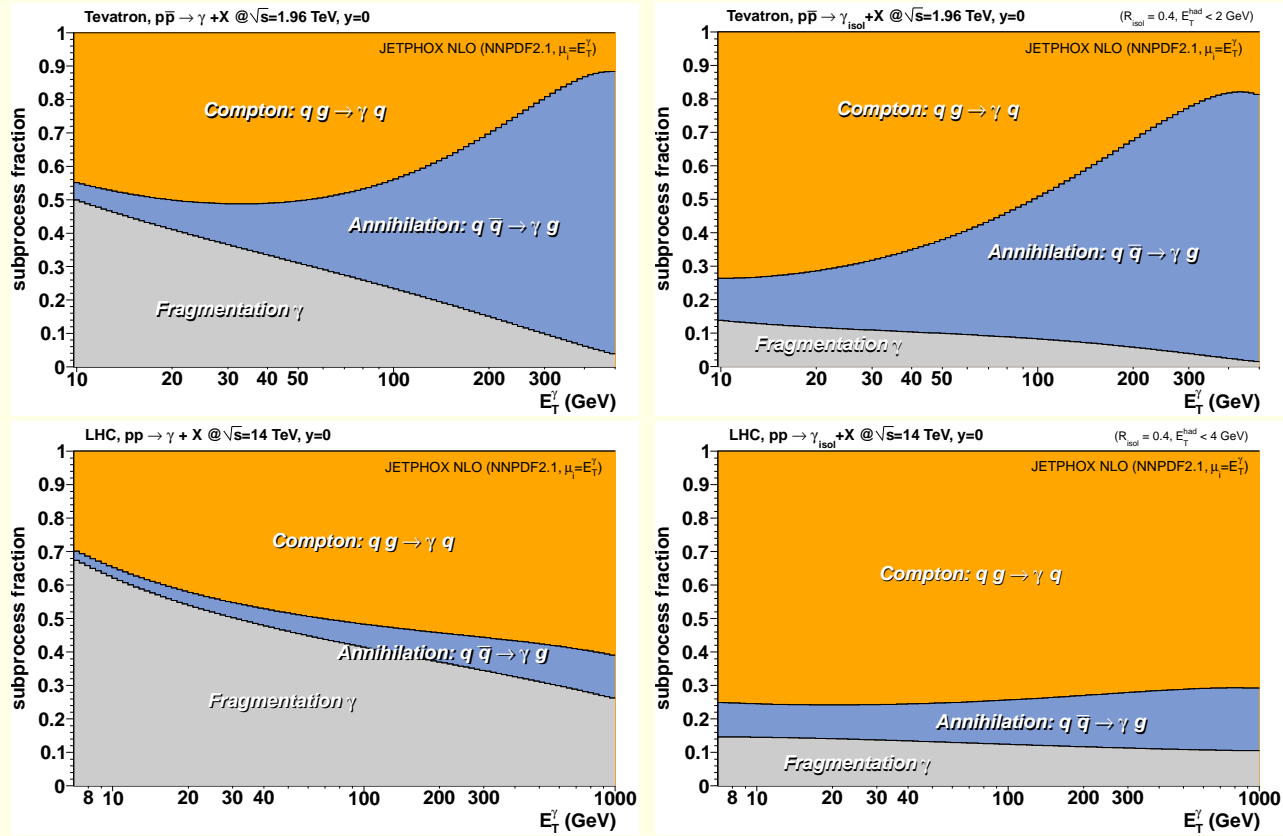
- Expect $p_T^4 E \frac{d^3\sigma}{dp^3}$ to be a function of x_T for fixed values of rapidity, purely on dimensional grounds
- Running coupling and PDF scale dependence modifies this to $n \approx 4.5$

Kinematic Coverage



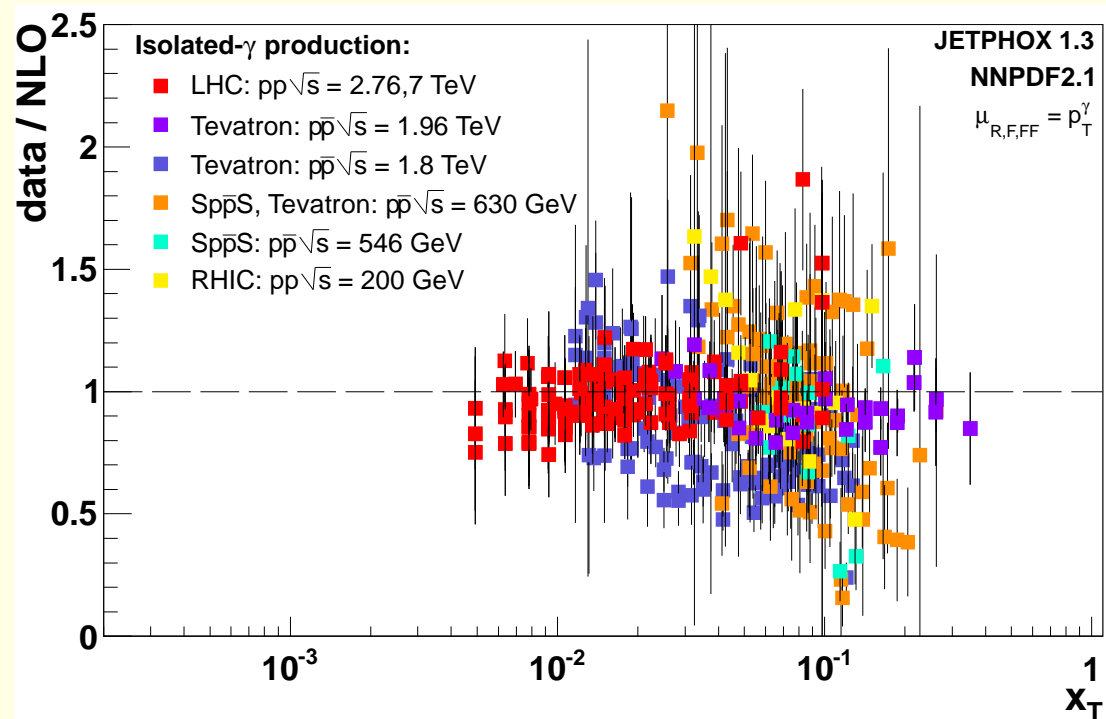
Compare kinematic coverage with that from DIS, lepton pair production, and collider jet data

Effects of Isolation Cuts



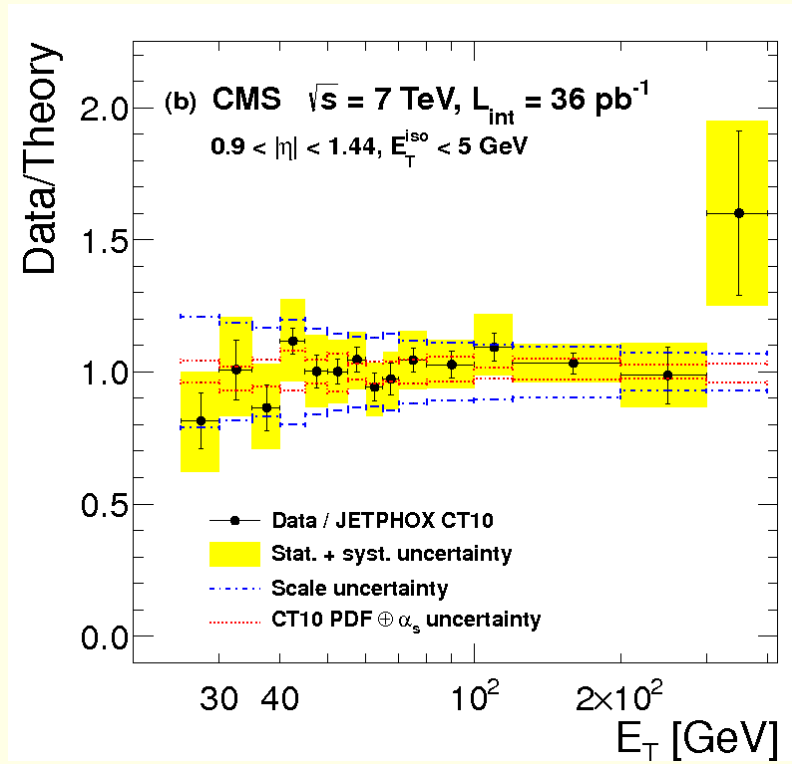
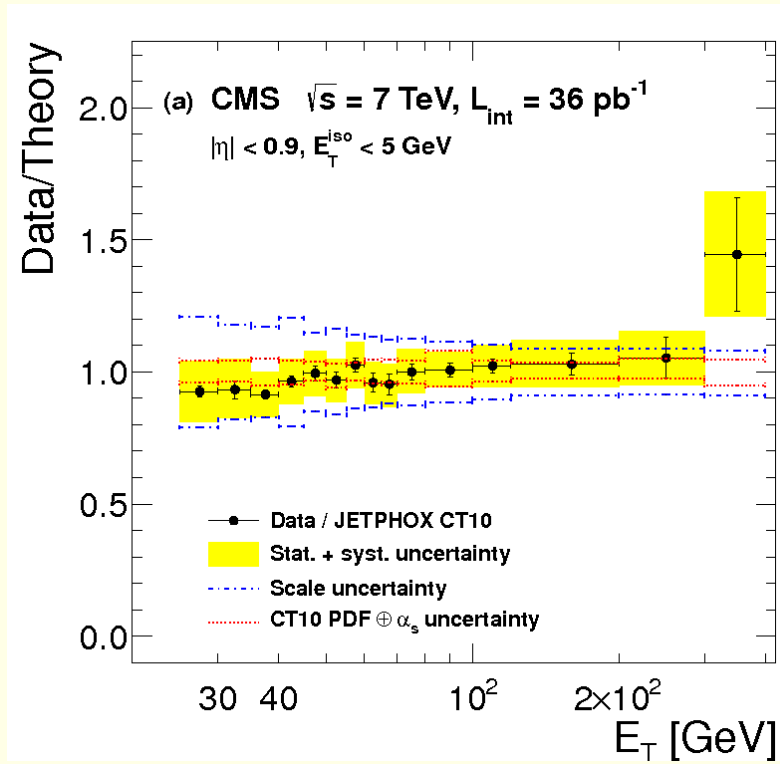
- Note reduced role of the annihilation subprocess at the LHC
- Note reduced contribution from fragmentation for the isolated cases

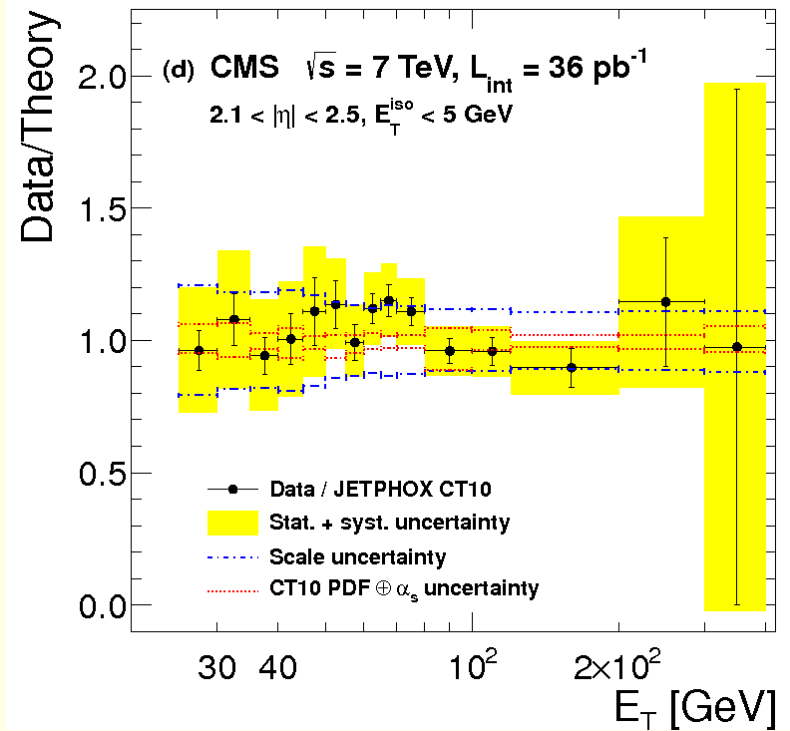
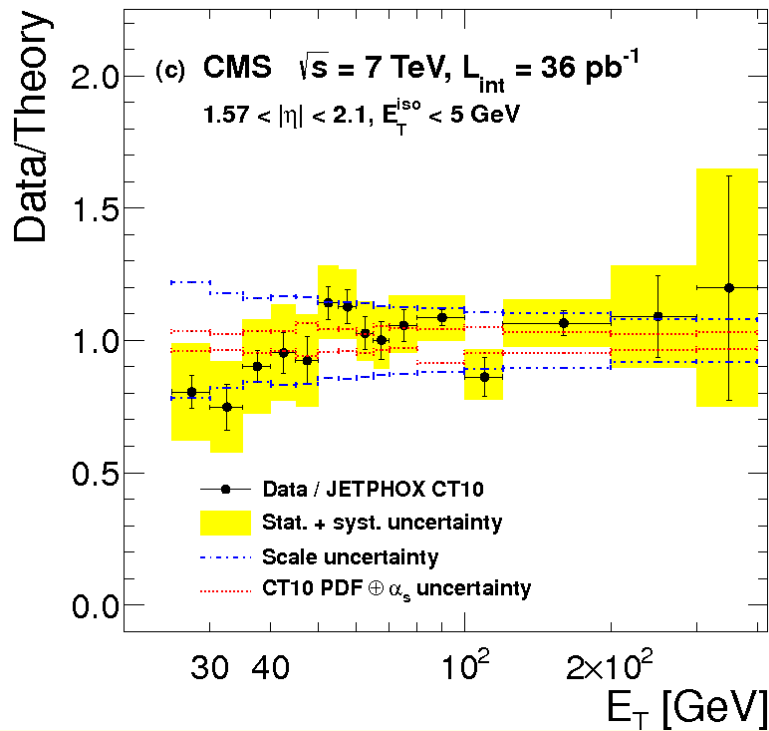
Comparison to theory



- Broad agreement between theory and experiment
- Some spread can be seen for the Tevatron and SPS collider data

First, look at results from CMS (arXiv:1108.2044)

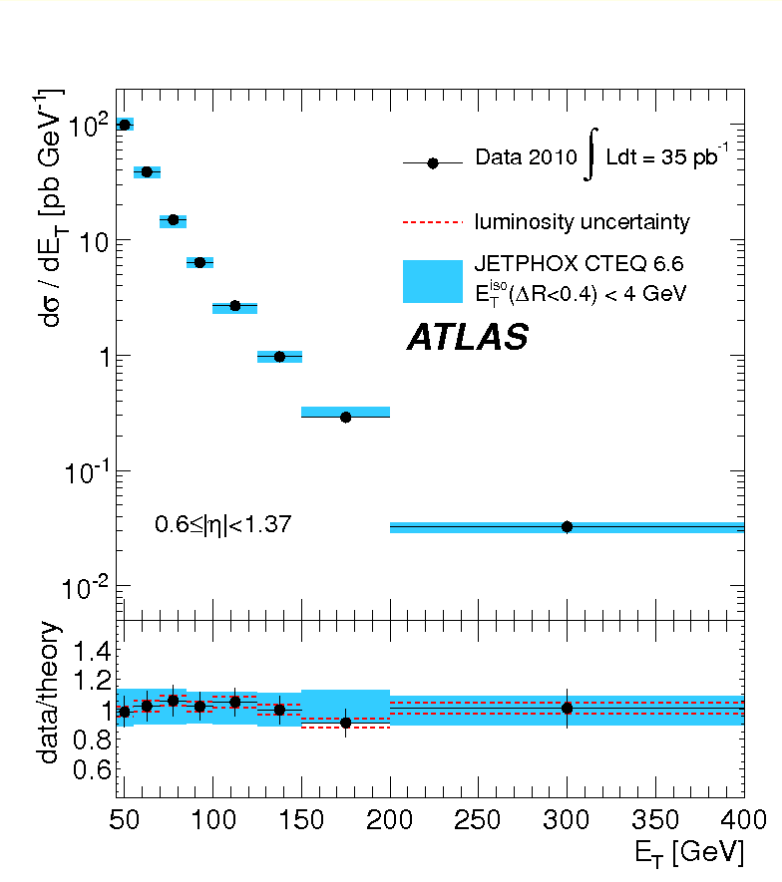
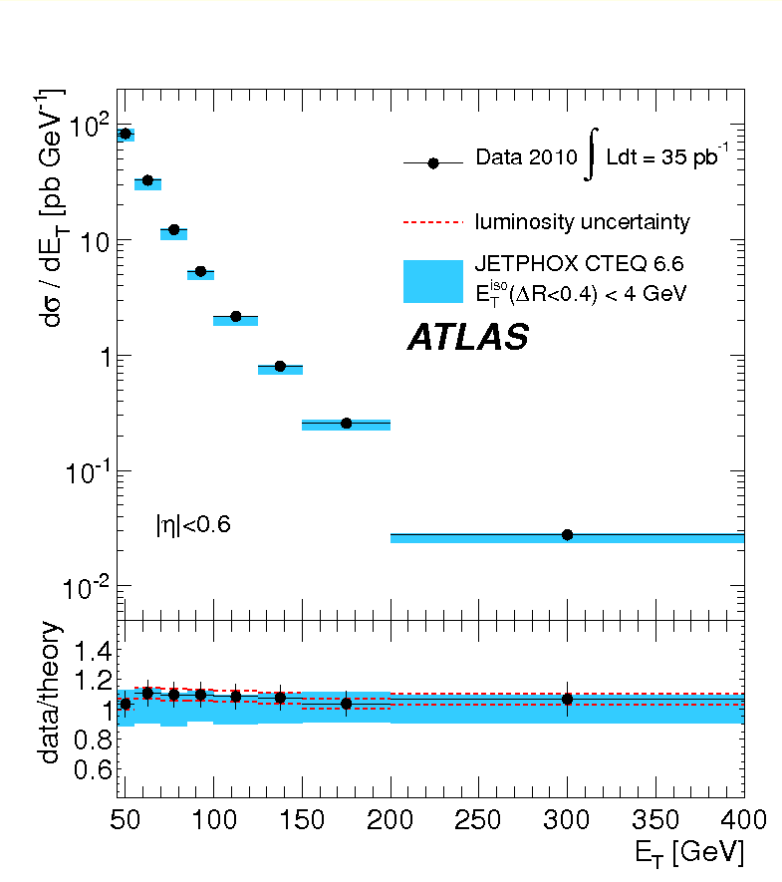


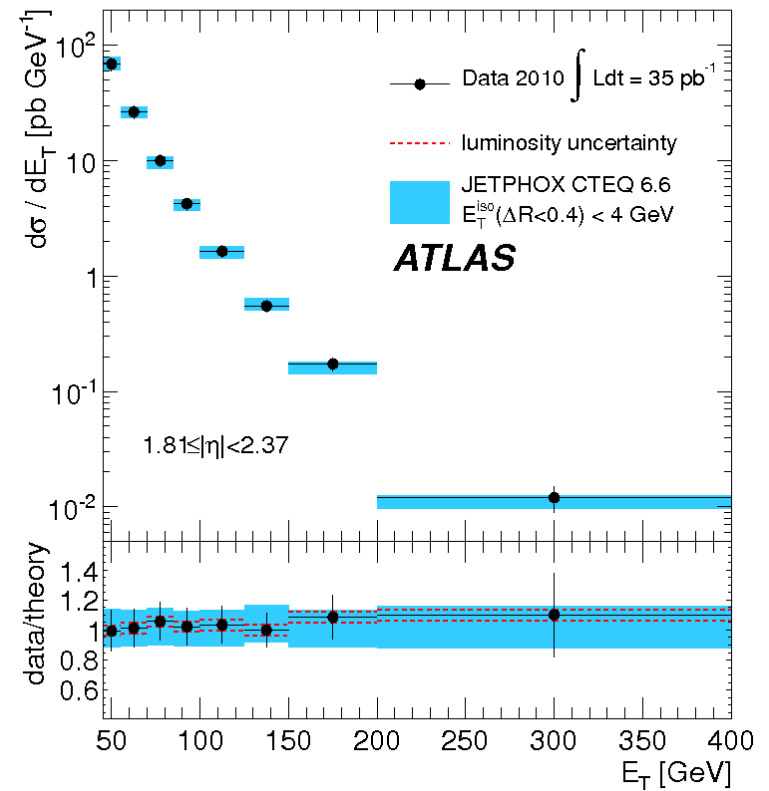
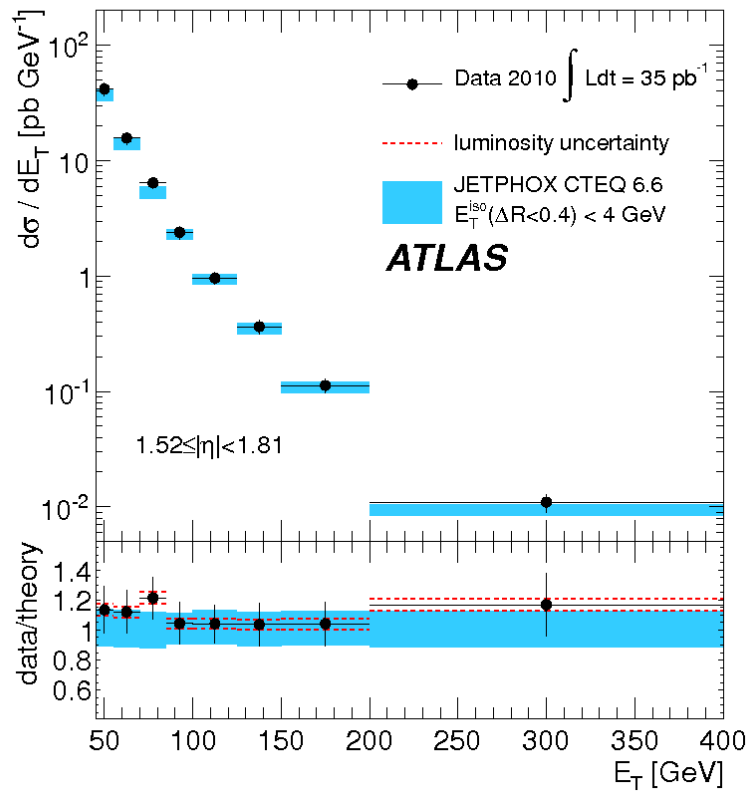


Data/theory plots show good agreement over the whole p_T range

- $25 < p_T < 400$ GeV/c
- $0.007 < x_T < 0.114$

ATLAS results (arXiv:1108.0253)

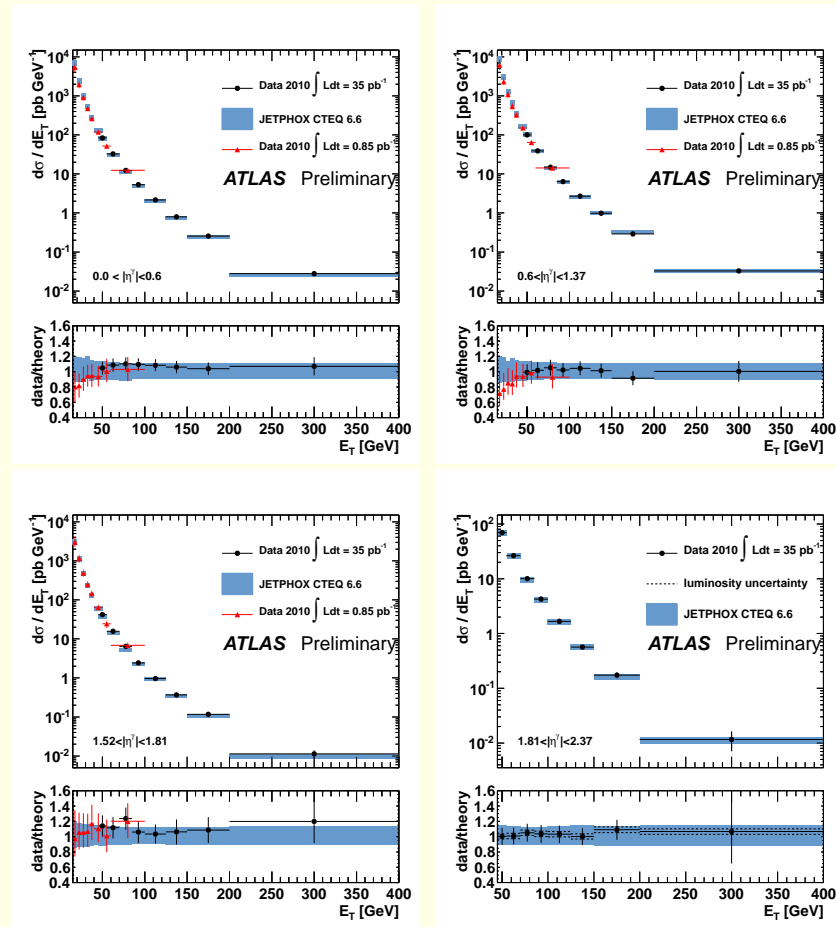




Again, good agreement seen for the data/theory ratio

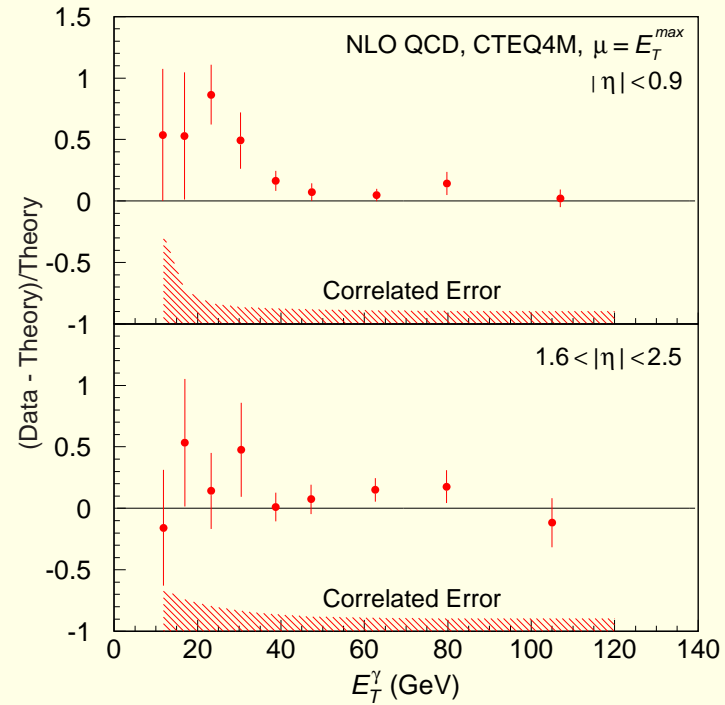
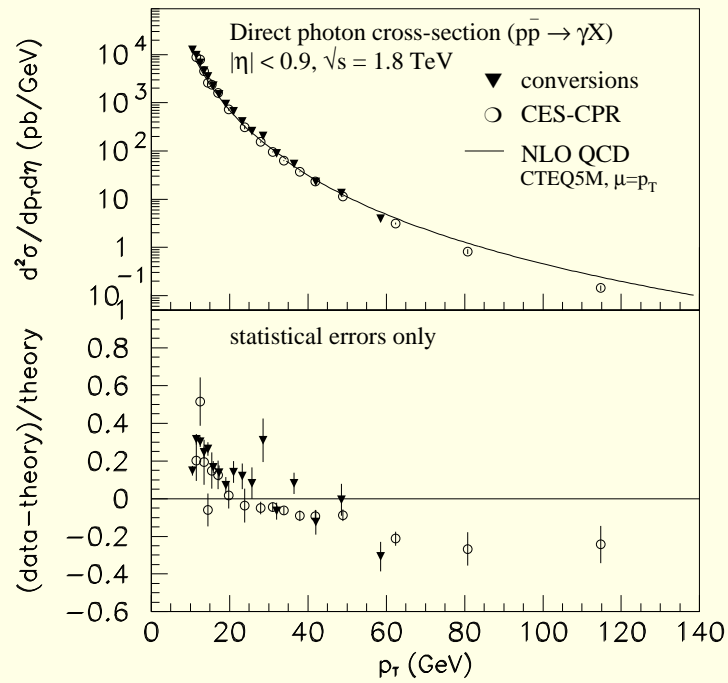
- $50 < p_T < 400 \text{ GeV}/c$
- $0.014 < x_T < 0.114$

Earlier ATLAS data (arXiv:1107.2200) extends to lower p_T values



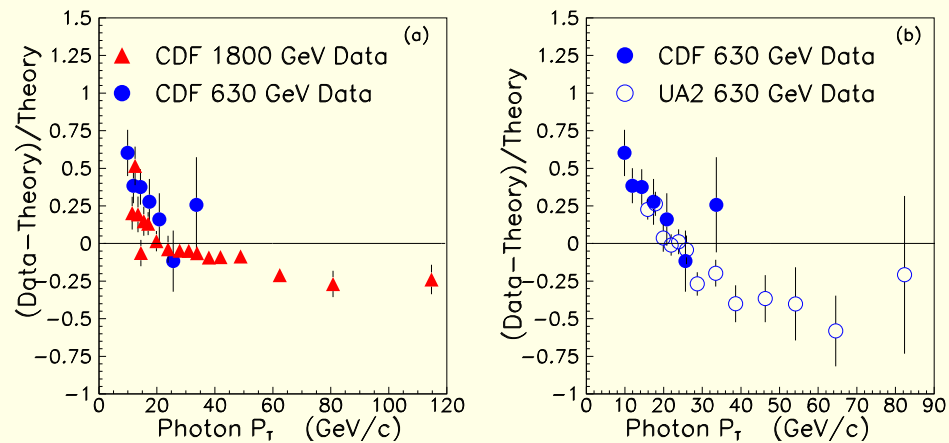
Note excess of theory over data below $p_T = 50$ GeV

Next, look at results from the Tevatron

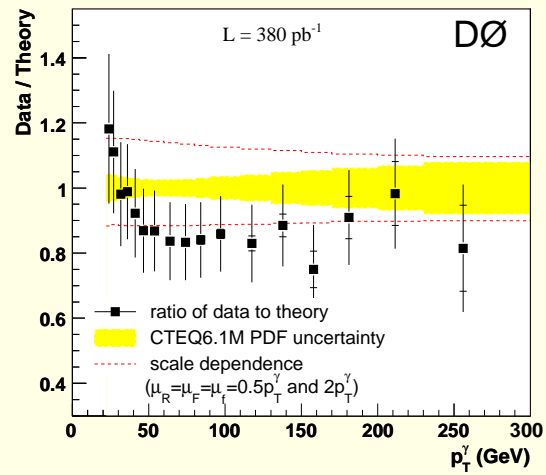
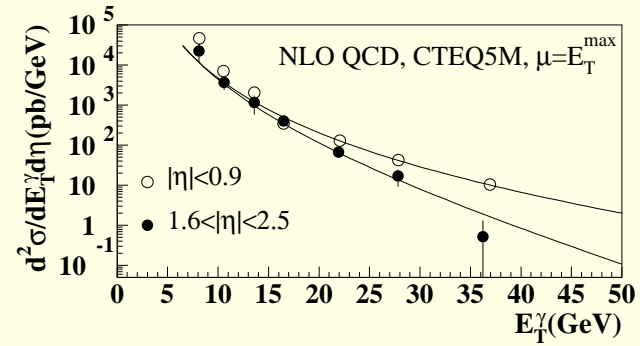
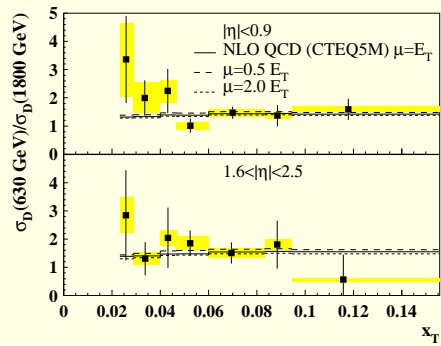


Both CDF and DØ see an excess of data over theory at the low p_T end in the central region

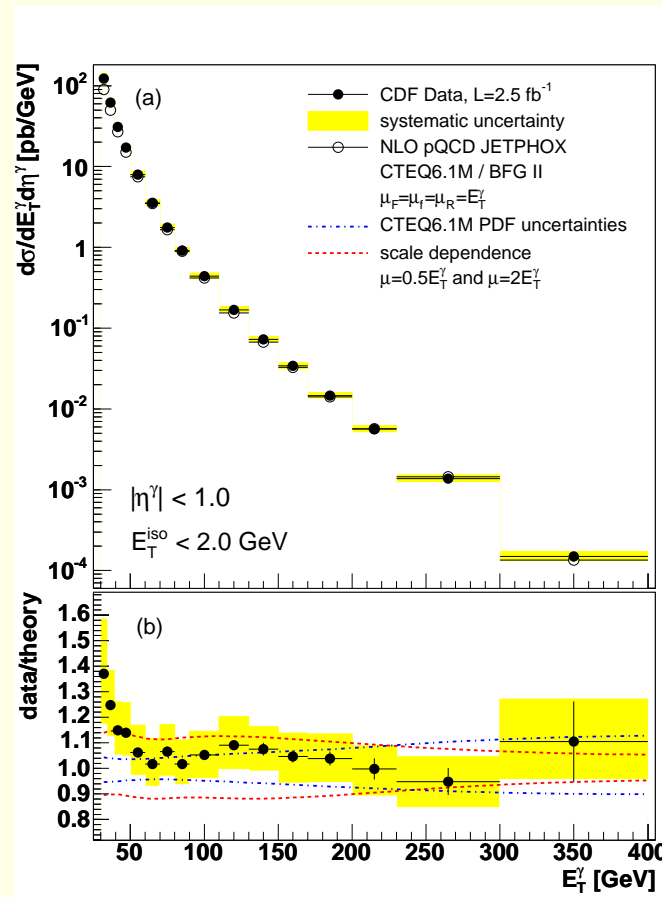
- Problem seen by CDF at both 1800 and 630 GeV
- Excess occurs at low p_T , not at fixed x_T , so the solution can not be a simple adjustment of the pdfs
- Effect also seen by UA-2



Also seen by DØ at 630 and 1960 GeV

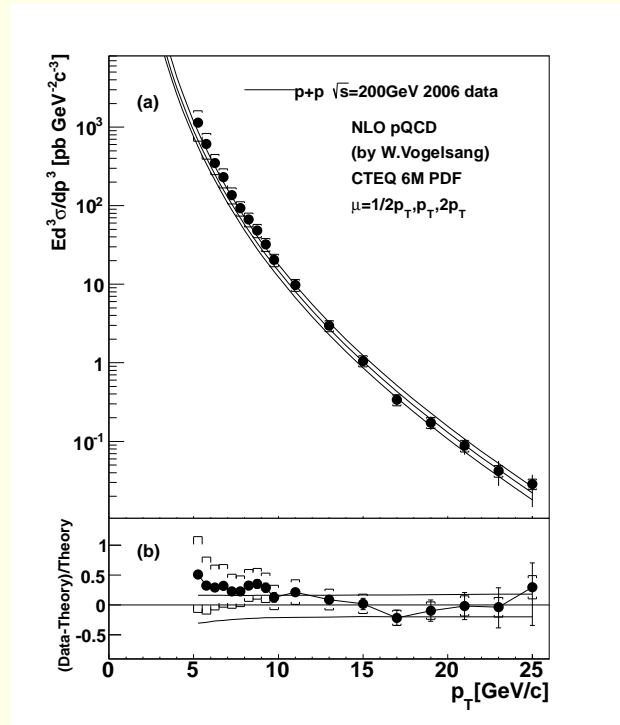


Latest Run II CDF data shows the same effect



Effect appears below about 50 GeV transverse momentum - agreement is good above that

Results from the PHENIX experiment (arXiv:1205.5533)



- Comparison is to the inclusive spectra - no isolation cuts
- Data and theory are consistent within errors
- No conclusive indication of an excess at low p_T

Comments

- Good agreement seen over the covered p_T range at $\sqrt{s} = 200$ and 7000 GeV
- Excess at the low p_T end seen at $\sqrt{s} = 630, 1800,$ and 1960 GeV
- Overlapping regions in x_T : $p_T = 20$ GeV/c at the Tevatron and $p_T = 70$ GeV/c at the LHC (7 TeV) both correspond to $x_T = .02$
- Explanation can not be ascribed to PDFs
- Unlikely to be due to modelling the isolation cuts because of the rapid p_T dependence seen for the excess

Photon-jet correlations and angular distributions

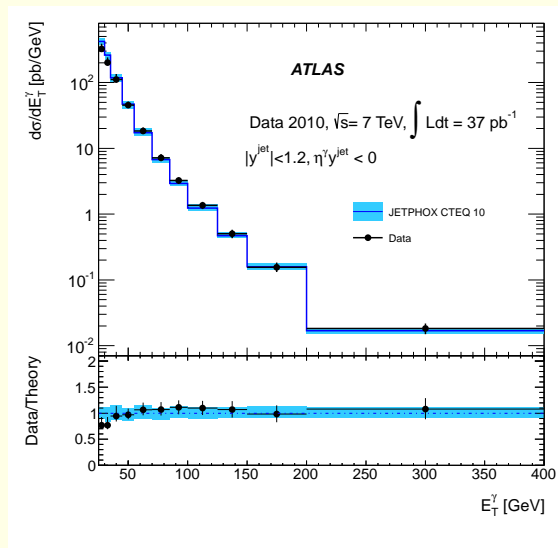
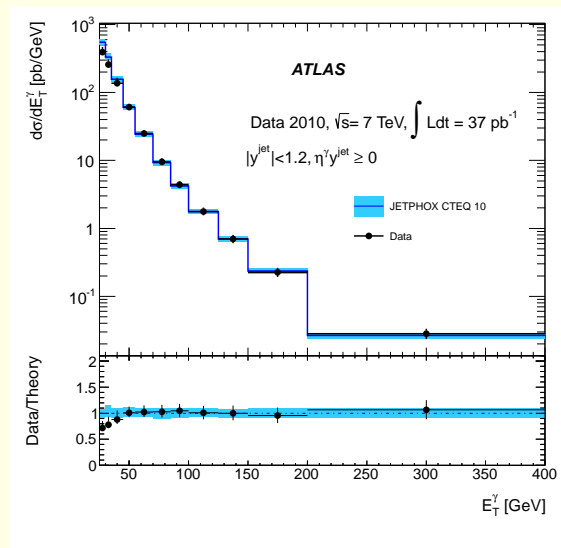
- If both the photon and the recoiling jet are measured, then one can test the underlying partonic subprocesses
- Using two-body kinematics, one has

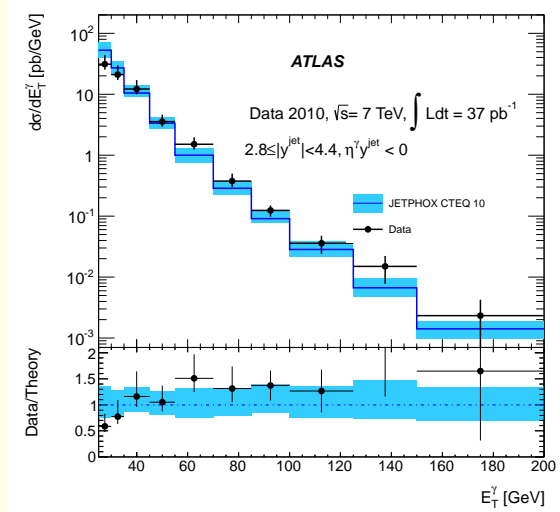
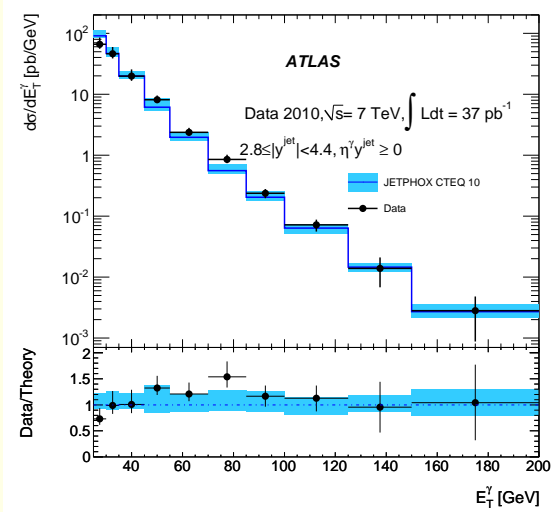
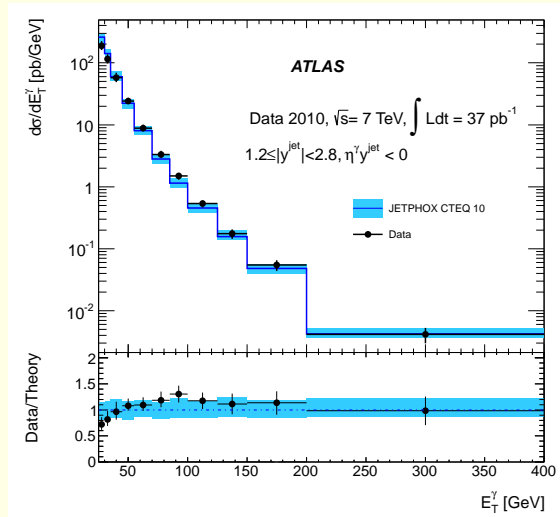
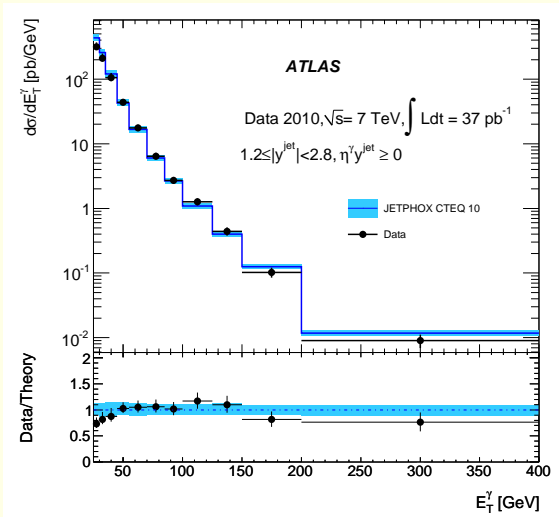
$$x_{a,b} = \frac{p_T}{\sqrt{s}} [e^{\pm\eta_\gamma} + e^{\pm y_{jet}}]$$

- Also, $\cos \theta^* = \tanh \frac{\eta_\gamma - y_{jet}}{2}$
- Expect flatter $\cos \theta^*$ distribution for γ production than for hadronic jet production (See the derivation in the Appendix)

ATLAS results for the photon plus jet cross section (arXiv:1203.3161)

- $|\eta_\gamma| < 1.37$
- Photon and jet in the same ($\eta_\gamma y_{jet} > 0$) or opposite ($\eta_\gamma y_{jet} < 0$) hemisphere



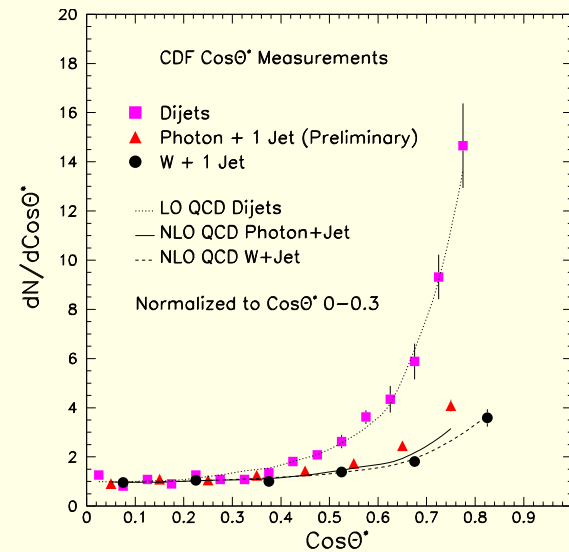
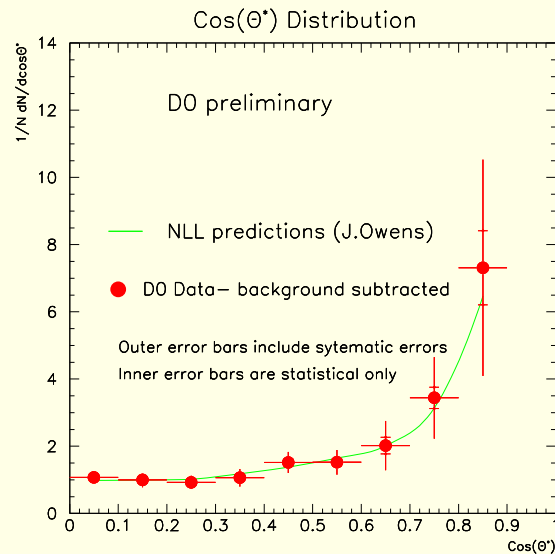


Comments

- All six regions show good agreement between theory and experiment
- Implies that the underlying subprocesses have the correct angular behavior
- Note that there appears to be an excess of **theory** over **data** for $p_T < 45$ GeV as shown earlier for the ATLAS single photon cross section data

Direct Measurement of the γ -jet angular distribution

- Measuring both η_γ and η_{jet} allows one to reconstruct $\cos\theta^* = \tanh\left(\frac{\eta_\gamma - \eta_{jet}}{2}\right)$
- Both DØ and CDF have measured the γ -jet angular distribution



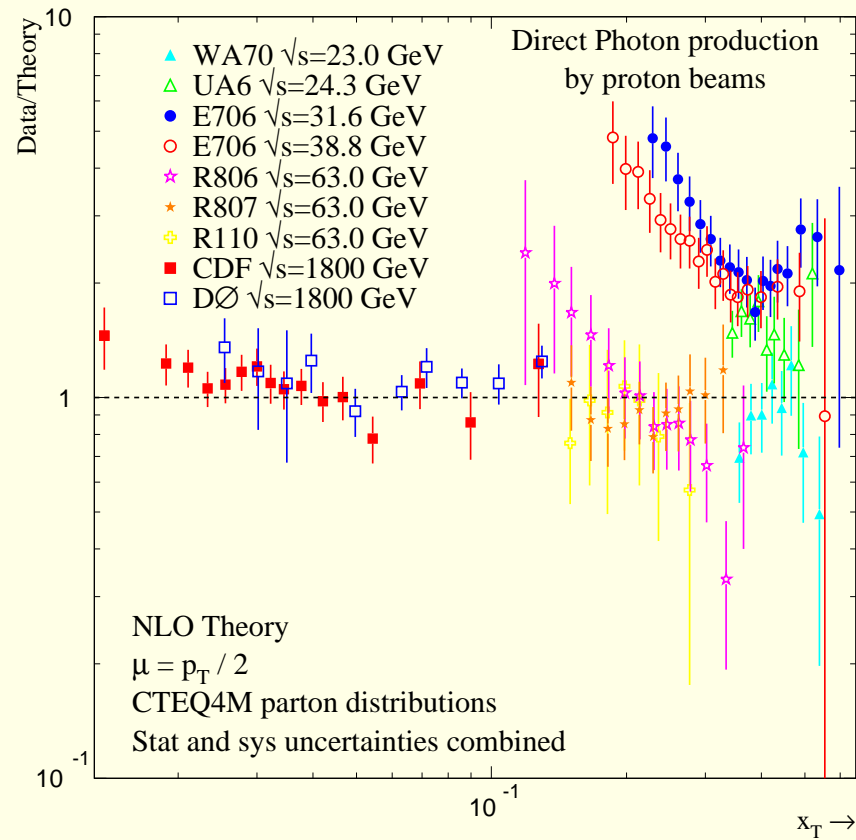
- Both experiments observe a shape consistent with expectations
- Direct photon production is dominated by subprocesses which yield a flatter angular distribution than is observed for dijet production

Comments

- Good agreement seen between theory and experiment over a wide range of energies, p_T s, and rapidities
- Some excesses or deficits in theory over experiment seen by some experiments at the low p_T end of the spectrum
- Photon-jet correlations and angular distributions appear to be in agreement with the theory
- High energy collider data are restricted to modest values of x_T , at least until additional statistics become available
- One motivation for studying photon production was to constrain the gluon PDF, especially at large values of x
- This region is probed by fixed target experiments at lower values \sqrt{s}

Fixed Target and Lower Energy Collider Data

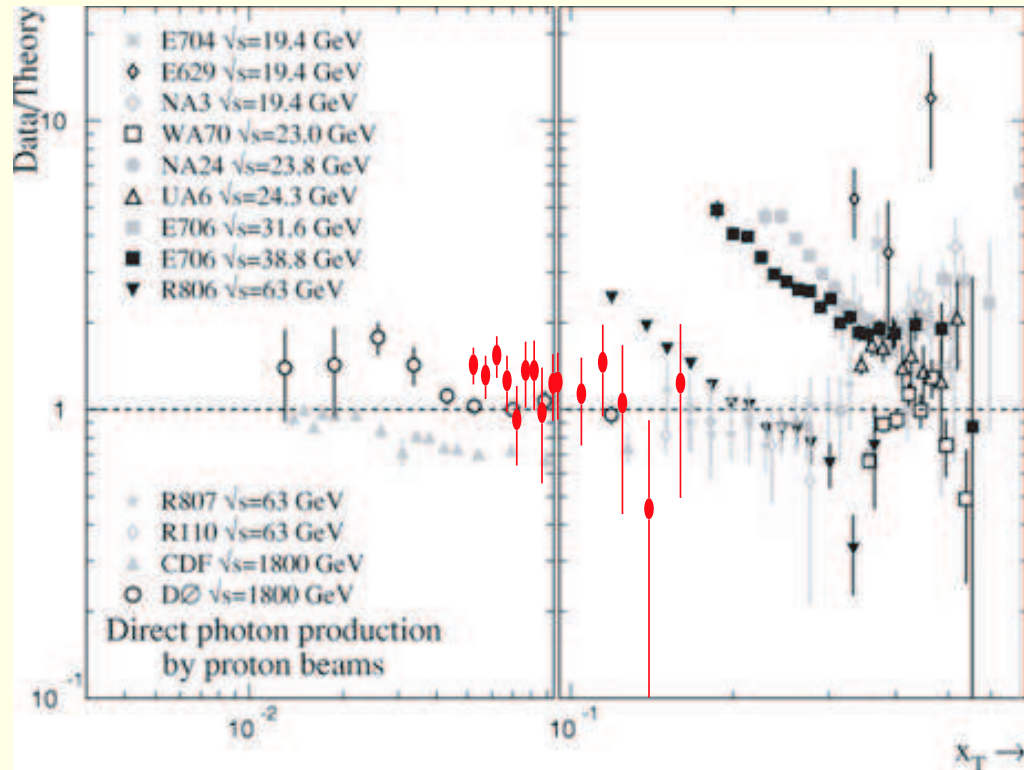
It is now time to consider the situation for the inclusive cross section at lower energies



Comments

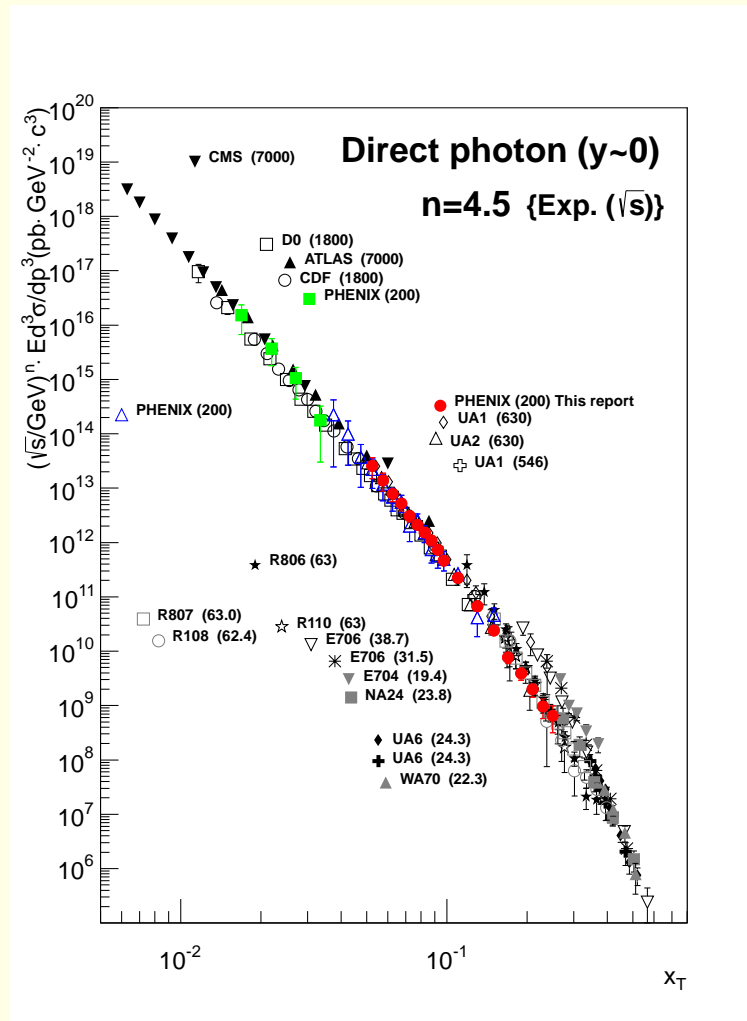
1. Data/Theory plotted versus x_T
2. Data plotted at same x_T but different \sqrt{s} correspond to different p_T 's
3. E706 higher than theory, UA6 somewhat above theory, WA70 and theory agree
 - Likely that there is some experimental inconsistency here since the range in \sqrt{s} is relatively small and it would take a significant modification of the theory to explain all three sets simultaneously.
4. See some shape disagreements among the ISR experiments
5. Plotted on this scale, the previously noted deviations of the theory from the CDF and DØ data look pretty darned small!

- Similar plot showing PHENIX data (nucl-ex/0504013)



- Agreement is comparable to that for other collider experiments and better than for the fixed target regime

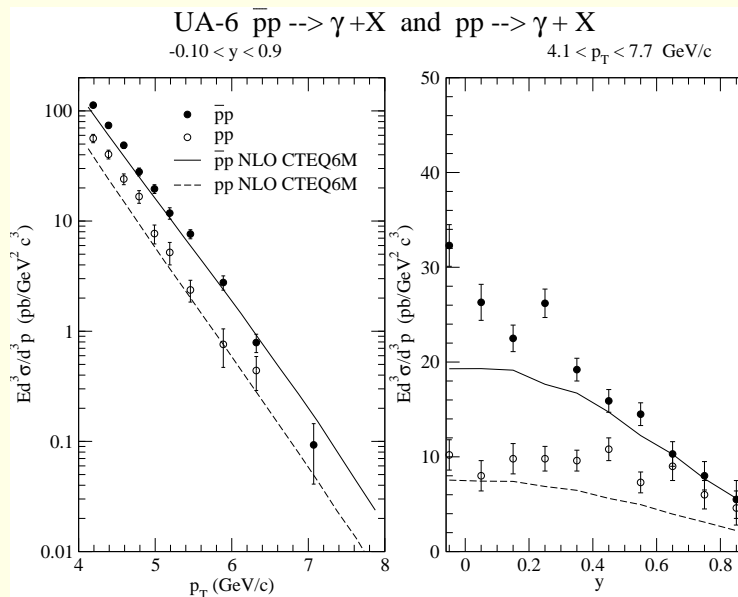
Another x_T scaling plot from airXiv:1205.5533 (PHENIX Collaboration)



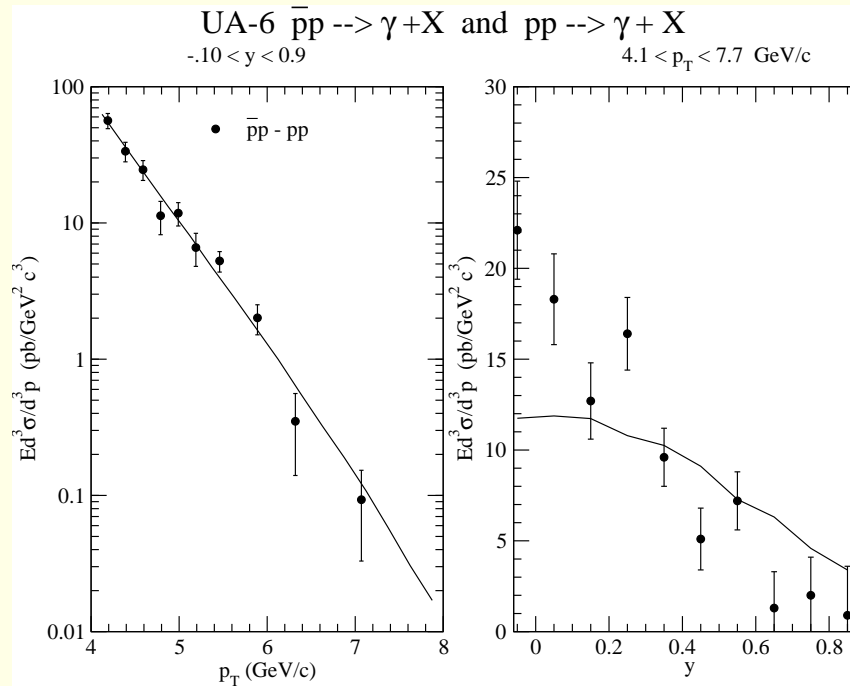
Shows consistency of collider data and the spread amongst the fixed target results

Example - UA-6

- Measured both pp and $\bar{p}p$ at $\sqrt{s} = 24.3 \text{ GeV}/c$
- Initial state gluon and gluon fragmentation contributions cancel in the $\bar{p}p - pp$ difference



- Theory below the data at the lower end of the p_T range
- Rapidity theory curves are flatter than the data



- Cross section difference cancels contributions from gluons
- p_T difference is well described
- Rapidity theory curve is somewhat flatter than the data
- So, the situation is mixed - the $\bar{p}p$ and pp curves are individually below the data, the p_T difference is well described, while the rapidity difference curve is a bit too flat

So what is going on?

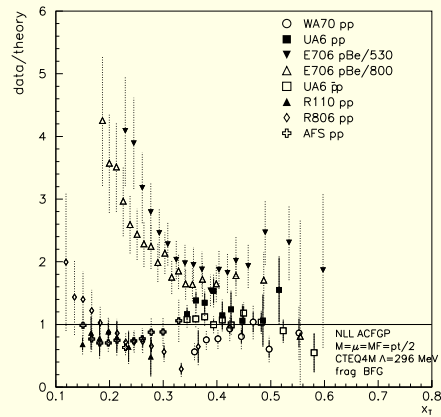
- Theory and data have different shapes for $\sqrt{s} = 630, 1800$ GeV with the theory being flatter than the data
- Some of the lower energy experiments show this same behavior to an even larger degree - others do not
- Critical review of the situation for the lower energy experiments: Aurenche, Fontannaz, Guillet, Kniehl, Pilon, and Werlen, hep-ph/9811382

Is this behavior seen for any other processes?

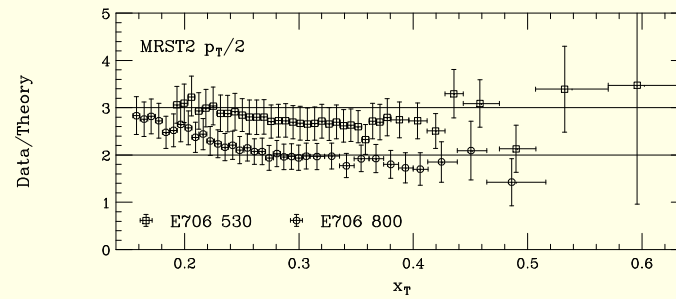
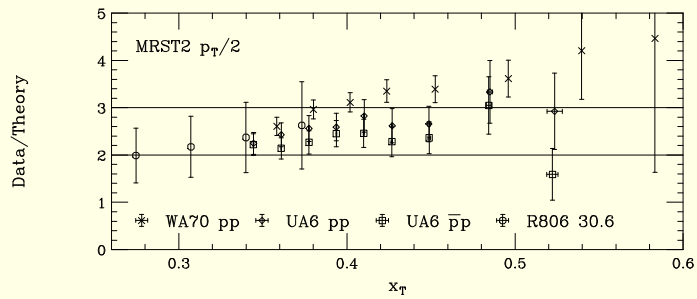
Yes - Inclusive single hadron production!

- Situation reviewed by Aurenche, Fontannaz, Guillet, Kniehl, and Werlen, hep-ph/9910252

Example plot for direct photon production

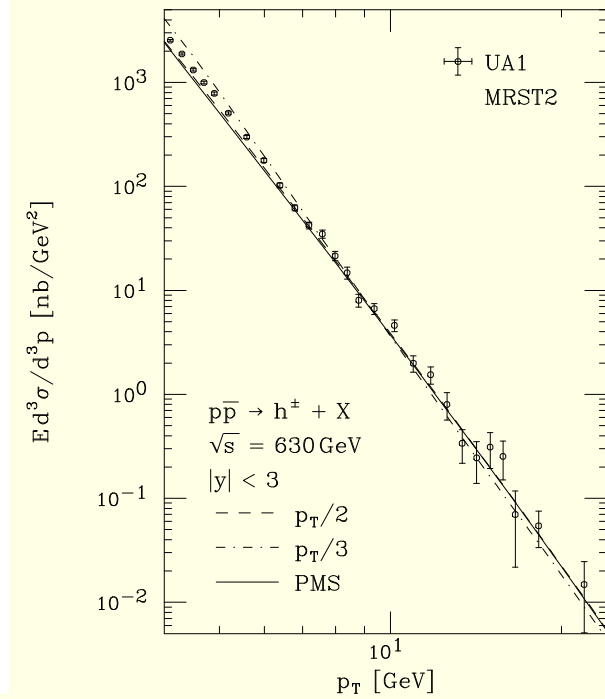
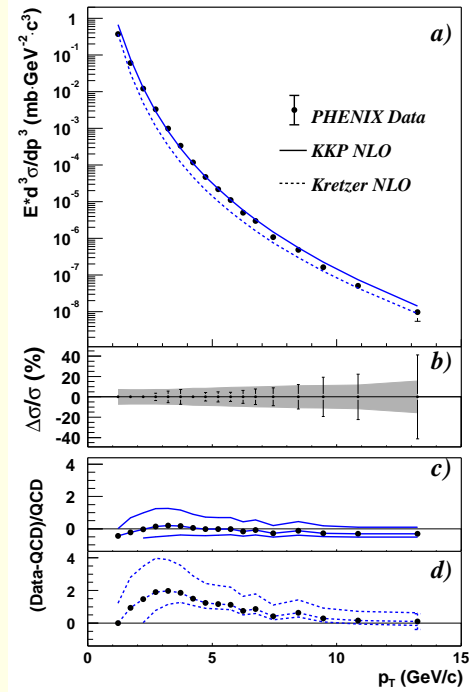
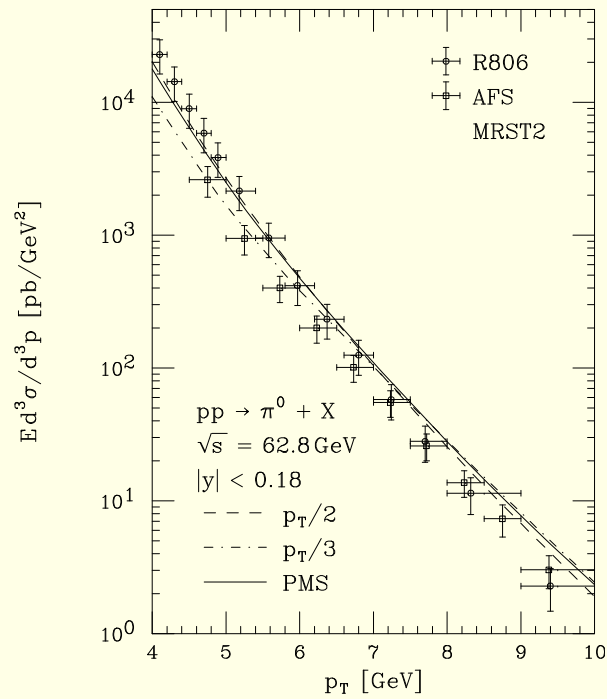


And two for π^0 production



See similar excesses of data over theory

But a strange thing happens as one goes up in energy...



Agreement between theory and data gets better at higher energies *and at lower p_T 's!*

So where do we stand?

1. Situation with fixed target direct photon production is confused by some disagreement between experiments
 - ▷ See Apanasevich et al., hep-ph/0007191 for a discussion of the systematics of γ/π^0 ratios and consistency between experiments
2. All experiments see an excess of data over theory for single hadron inclusive production at fixed target energies
3. Agreement between theory and data for single hadron production improves with increasing energy and is excellent by $\sqrt{s} = 200$ GeV
4. Likely that we need an *improved method of calculating single particle inclusive cross sections* in the fixed target energy range - one that would improve agreement for both photon and hadron production
5. A reassessment of systematic errors on the existing fixed target photon experiments might also help resolve the discrepancies between data sets

Theoretical Ideas and Scenarios

Start by considering the case of single hadron production where all experiments in the fixed target regime see an excess of data over theory

- The steeply falling spectra in the fixed target region force the fragmentation variable z to be near one. As one goes up in energy the distributions flatten somewhat and $\langle z \rangle$ decreases
- Fragmentation functions are not well constrained by data at high values of z
- Fragmentation functions behave as $(1 - z)^n$ with $n \approx 2 - 3$.
- As $z \rightarrow 1$ large logarithms of $(1 - z)$ should be resummed

Resummation may offer a way of significantly increasing the fixed target predictions ($\langle z \rangle$ near 1) while not raising the already successful higher energy predictions too much (here $\langle z \rangle \ll 1$)

Threshold Resummation

Basic Physics -

- For inclusive calculations singularities from soft real gluon emission cancel against infrared singularities from virtual gluon emission
- Limitations on real gluon emission imposed by phase space constraints can upset this cancellation
- Singular terms still cancel, but there can be large logarithmic remainders
- Classic example is thrust distribution in $e^+e^- \rightarrow jets$
- For hadronic reactions with PDFs and FFs the collinear factors actually conspire to enhance the partonic cross sections (See my resummation lecture at the 2010 CTEQ school)

High- p_T particle production

- For typical fixed target energies the PDFs are evaluated at rather large x values and the fragmentation functions are evaluated at large z
- For example, $\sqrt{s} = 30$ GeV and $p_T = 7.5$ GeV gives $x_T = .5$
- Steeply falling PDFs and fragmentation functions constrain real gluon emission when high- p_T is required since it costs a significant amount of the parton-parton center-of-mass energy to emit additional partons beyond the one that is fragmenting into the observed hadron.
- Phase space for gluon emission is limited near kinematic threshold in the parton-parton scattering subprocess for producing the hadron with the observed value of p_T

Define $v = 1 + t/s$ and $w = -u/(s + t)$.

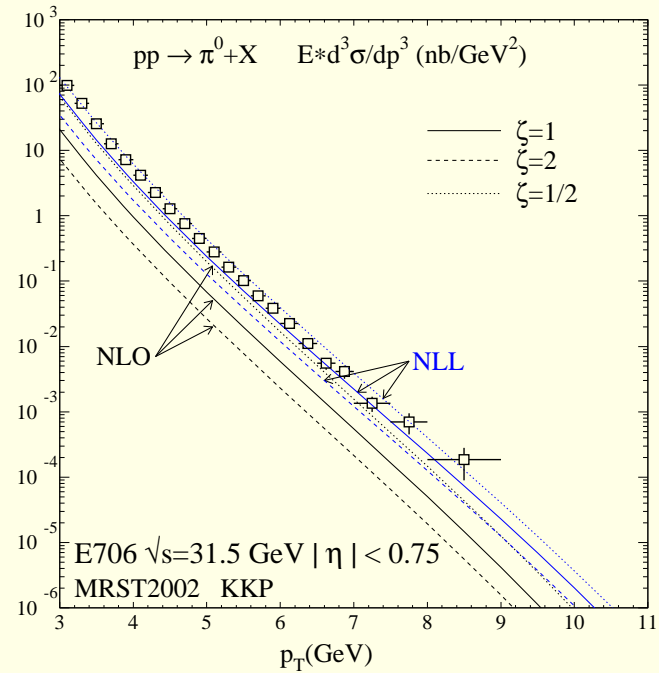
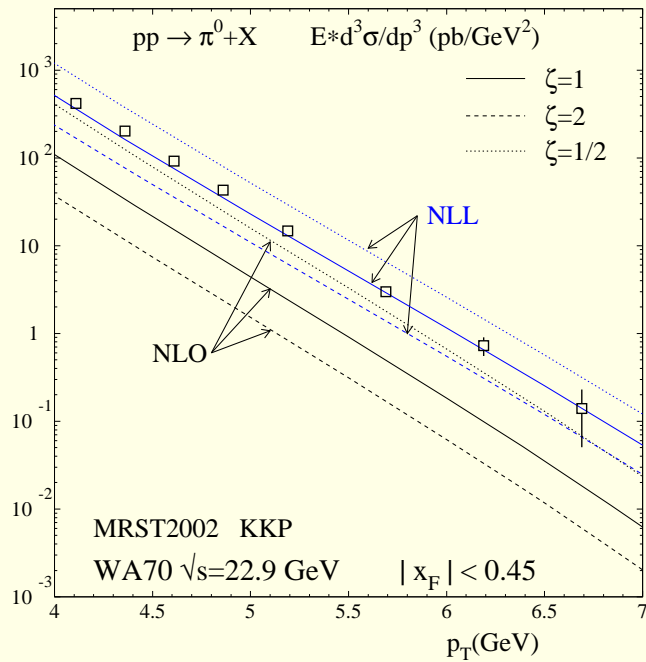
Threshold occurs at $w = 1$ ($s + t + u = 0$)

Soft gluon emission gives rise to terms in the partonic cross sections which behave like $\alpha_s^m \left(\frac{\ln^n(1-w)}{1-w} \right)_+$ relative to the Born terms which are $\mathcal{O}(\alpha_s^2)$ in this case.

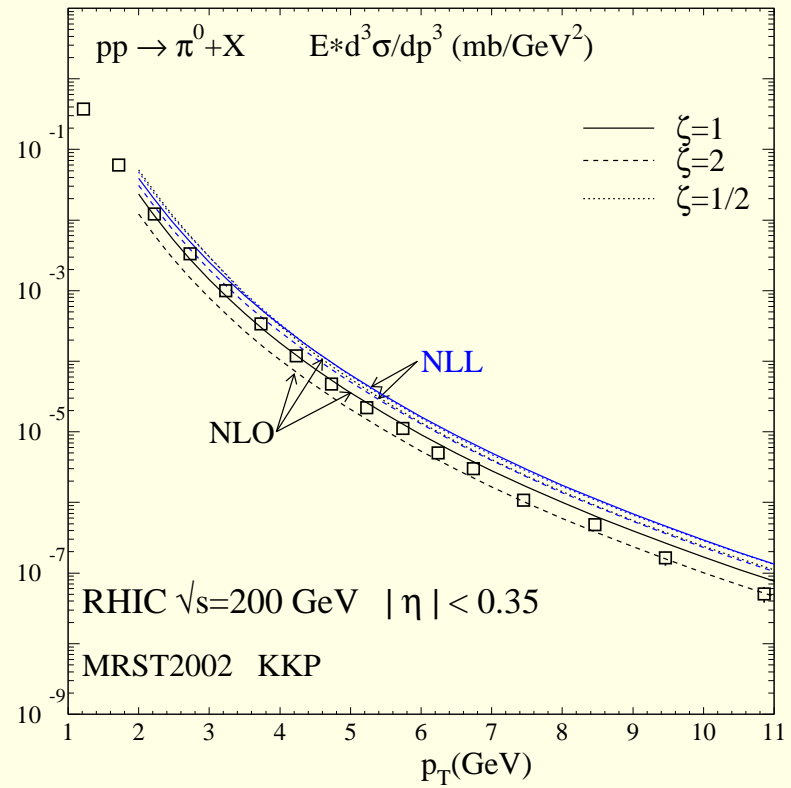
Can sum leading logs ($n = 2m - 1$), next-to-leading-logs ($n = 2m - 2$), etc.

Application to the π^0 cross section

- Paper by de Florian and Vogelsang (hep-ph/0501258) applies threshold resummation to π^0 production
- Large values of the fragmentation variable z relevant for fixed target energies leads to large threshold resummation corrections there.
- Enhancement is strongly energy dependent since the relevant values of z decrease as one goes to higher energies at fixed p_T .
- Enhancement is larger than that observed in jet production since the jet cross section doesn't involve fragmentation functions



- Blue curves include the resummation corrections properly matched to an existing NLO calculation in order to avoid double counting.
- Note the reduced scale dependence of the resummed results.



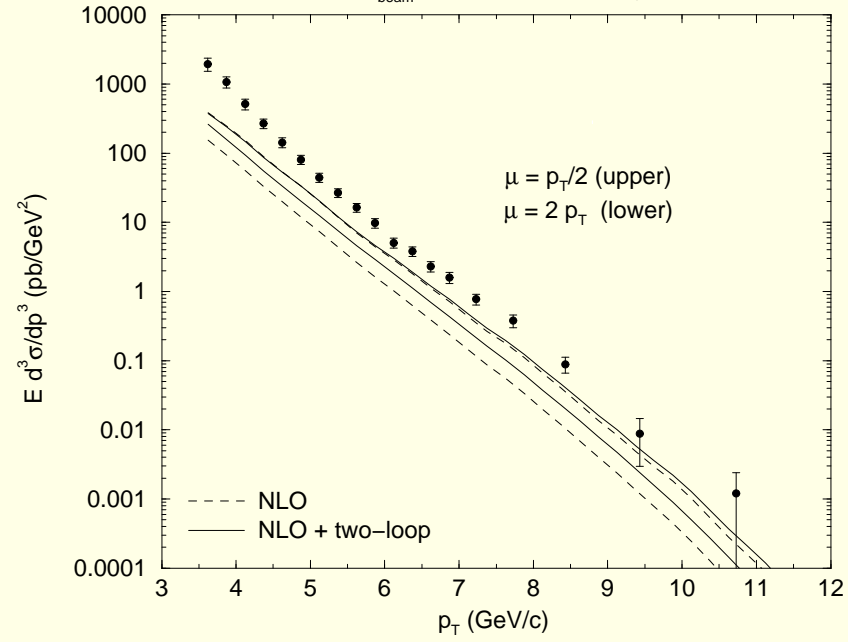
- Note reduced enhancement at RHIC energy compared to the previous fixed target results

What about direct photons? Can threshold resummation help?

- Example application to the fixed target data - N. Kidonakis and J.F. Owens, Phys. Rev. D61, 094004, 2000; hep-ph/9912388
- Fixed target region dominated by annihilation and Compton subprocesses
- Fragmentation doesn't play as large a role as at higher energies since it costs extra energy to have a photon produced by fragmentation
- No significant enhancement to the annihilation and Compton terms
- Reduced scale dependence observed

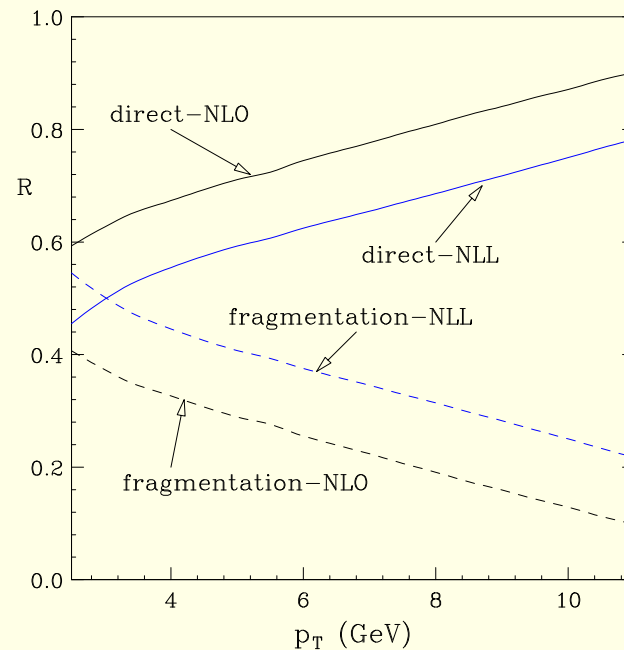
$p N \rightarrow \gamma + X$

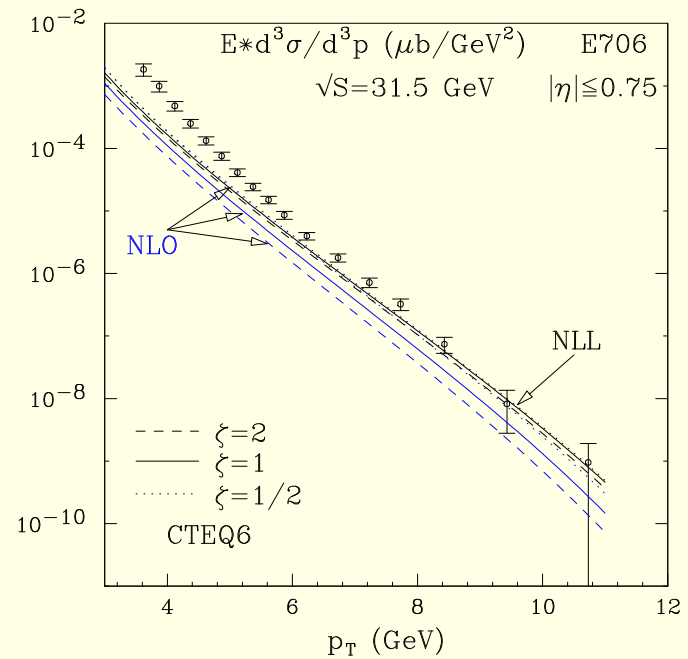
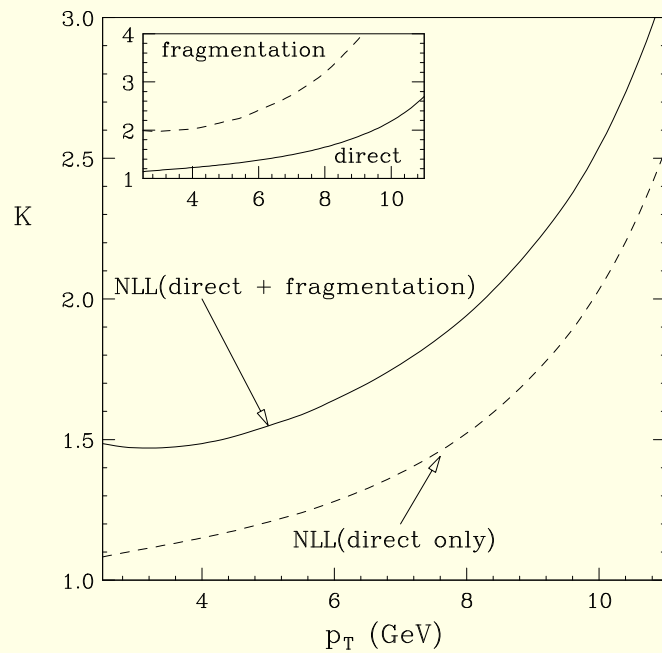
E-706 $p_{\text{beam}}=530 \text{ GeV}/c$ $-0.75 < y < 0.75$



But...

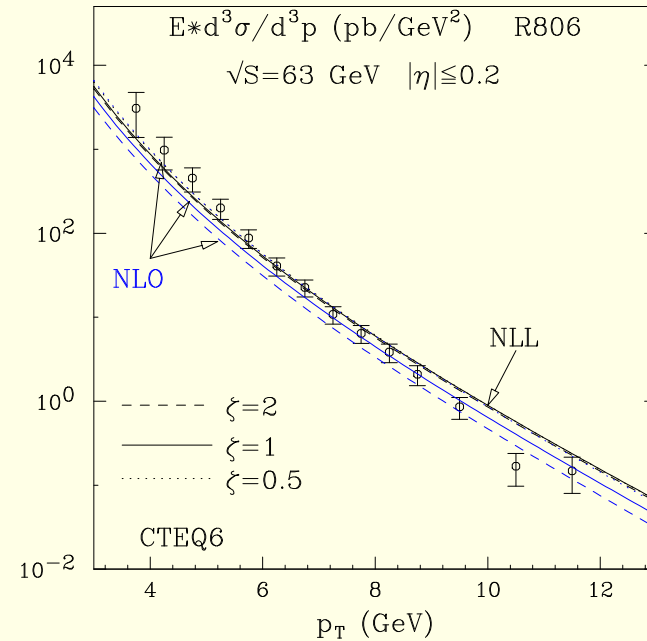
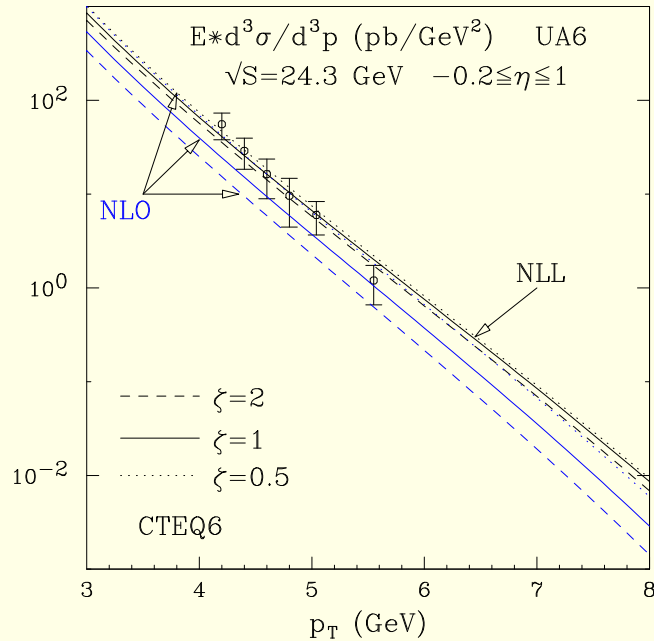
- The fragmentation contribution is *not* zero at fixed target energies
- Vogelsang and de Florian had previously shown that the fragmentation contribution in *hadro*production was significantly enhanced by threshold resummation
- They subsequently applied the formalism to direct photons in hep-ph/0506150
- Relative contribution of fragmentation versus direct *is* enhanced





- Resumming the fragmentation component results in a larger increase than if just the direct component is resummed
- Still isn't enough to describe the E-706 results

Resummation *can* result in a good description of the UA-6 pp data



- Fragmentation component largely cancels in the $\bar{p}p - pp$ difference, so the previous good agreement for this is retained
- Enhancement decreases rapidly with energy as in the hadroproduction case so that agreement with higher energy data is retained

Bottom line on threshold resummation

- Provides reduced scale dependence
- Provides an enhancement in the fixed target regime, but the effect is much smaller at higher energies
- Can improve the agreement with some fixed target experiments without adversely affecting the agreement at higher energies

Assessment

- A rather consistent picture seems to be emerging
 - For $p_T > 50$ GeV the Tevatron data from DØ and CDF are well described by the theory
 - At the LHC good agreement is seen over all p_T above 50 GeV
 - For the fixed target energy range, threshold resummation applied to both the direct and fragmentation components will help improve the agreement between theory and experiment while preserving the agreement with the collider data
- Both the DØ and CDF results show an excess of data/theory below p_T of 50 GeV or so
- Threshold resummation won't affect this region significantly
- Isolation cuts and the methods used to calculate their effects do not seem to be responsible as the isolation effects are not as large as the excess and the effects are rather smooth in p_T with no sharp onset
- Note that ATLAS shows an **overestimate** of the data below $p_T = 45$ GeV

Summary and Conclusions

1. Examining γ -jet observables suggests that high- p_T photons are produced in accordance with the expectations based on QCD
2. There is broad agreement between the theory and most experimental results for the photon p_T distribution
3. Threshold resummation has been shown to play an important role in hadroproduction at fixed target energies and can offer some improvement for direct photons
 - Enhances the fragmentation contribution more than was previously anticipated in the fixed target regime
 - Effects are reduced at collider energies as the since smaller values of x_T are probed

While there are a few remaining issues, the overall description of the data over nine orders of magnitude is encouraging

Appendix: some miscellaneous and hopefully useful stuff

1. Check out the CTEQ web page at www.cteq.org

- information on past summer schools, including transparencies of many of the lectures
- information and links for parton distributions
- CTEQ List of Challenges in Perturbative QCD
- CTEQ Pedagogical Page
- CTEQ Handbook of Perturbative QCD

2. Four-vectors and rapidity

- rapidity is defined as $y = \frac{1}{2} \ln \frac{E+p_z}{E-p_z}$. For massless particles this reduces to the pseudorapidity which is defined as $\eta = \ln \cot \theta/2$.
- the four-vector for a massless particle with transverse momentum p_T and rapidity y may be conveniently expressed as

$$p^\mu = (p_T \cosh y, p_T, 0, p_T \sinh y)$$

3. Mandelstam variables

- For a two-body process $p_1 + p_2 \rightarrow p_3 + p_4$ the three Mandelstam variables are defined as

$$s = (p_1 + p_2)^2$$

$$t = (p_1 - p_3)^2$$

$$u = (p_1 - p_4)^2$$

- For processes with more particles one sometimes encounters variables such as $s_{ij} = (p_i + p_j)^2$ which is just the squared invariant mass of particles i and j and $t_{ij} = (p_i - p_j)^2$ which is the squared four-momentum transfer between particles i and j .

4. Another example: direct photon production $qg \rightarrow \gamma + q$

- four-vectors in the hadron-hadron center-of-mass frame

$$p_q = \frac{\sqrt{s}}{2} x_a (1, 0, 0, 1)$$

$$p_g = \frac{\sqrt{s}}{2} x_b (1, 0, 0, -1)$$

$$p_\gamma = p_T (\cosh y, 1, 0, \sinh y)$$

- Substituting these four-vectors into the expressions for the Mandelstam variables above yields

$$\hat{s} = x_a x_b s$$

$$\hat{t} = -x_a p_T \sqrt{s} e^{-y}$$

$$\hat{u} = -x_b p_T \sqrt{s} e^y$$

- \hat{s} is often used to denote a variable at the parton level.

5. Convolutions

- The symbol \otimes is sometimes used to denote a convolution:

$$\begin{aligned} f \otimes g &= \int_0^1 dy \int_0^1 dz f(y) g(z) \delta(x - yz) \\ &= \int_x^1 \frac{dz}{z} f(x/z) g(z) \end{aligned}$$

6. Subprocesses and angular distributions

The two lowest order subprocesses for direct photon production are (in units of $\pi\alpha\alpha_s/\hat{s}^2$)

$$\begin{aligned}\frac{d\sigma}{d\hat{t}}(gq \rightarrow \gamma q) &= -\frac{e_q^2}{3} \left[\frac{\hat{u}}{\hat{s}} + \frac{\hat{s}}{\hat{u}} \right] \\ \frac{d\sigma}{d\hat{t}}(q\bar{q} \rightarrow \gamma g) &= \frac{8}{9}e_q^2 \left[\frac{\hat{u}}{\hat{t}} + \frac{\hat{t}}{\hat{u}} \right]\end{aligned}$$

The dominant parton-parton scattering subprocesses for hadroproduction are
(in units of $\pi\alpha_s^2/\hat{s}^2$)

$$\begin{aligned} \frac{d\sigma}{d\hat{t}}(qq' \rightarrow qq') &= \frac{4}{9} \left[\frac{\hat{s}^2 + \hat{u}^2}{\hat{t}^2} \right] \\ \frac{d\sigma}{d\hat{t}}(qg \rightarrow qg) &= -\frac{4}{9} \left[\frac{\hat{s}}{\hat{u}} + \frac{\hat{u}}{\hat{s}} \right] + \frac{\hat{s}^2 + \hat{u}^2}{\hat{t}^2} \\ \frac{d\sigma}{d\hat{t}}(gg \rightarrow gg) &= \frac{9}{2} \left[3 - \frac{\hat{t}\hat{u}}{\hat{s}^2} - \frac{\hat{s}\hat{u}}{\hat{t}^2} - \frac{\hat{s}\hat{t}}{\hat{u}^2} \right] \end{aligned}$$

- In the parton-parton center-of-mass frame, one can write

$$\begin{aligned}\hat{t} &= -\frac{\hat{s}}{2}(1 - \cos(\theta^*)) \\ \hat{u} &= -\frac{\hat{s}}{2}(1 + \cos(\theta^*))\end{aligned}$$

- Therefore, as $\cos(\theta^*) \rightarrow 1(-1)$, $\hat{t}(\hat{u}) \rightarrow 0$. Hence, in this limit, the first two subprocesses on the preceding page behave as $(1 - |\cos(\theta^*)|)^{-1}$ while the next three behave as $(1 - |\cos(\theta^*)|)^{-2}$.

7. Center of mass scattering angle

Start in the parton-parton center of mass frame where one has

$$\begin{aligned} p_1 &= \frac{\sqrt{\hat{s}}}{2}(1, 0, 0, 1) & p_2 &= \frac{\sqrt{\hat{s}}}{2}(1, 0, 0, -1) \\ p_3 &= \frac{\sqrt{\hat{s}}}{2}(1, \sin \theta^*, 0, \cos \theta^*) & p_4 &= \frac{\sqrt{\hat{s}}}{2}(1, -\sin \theta^*, 0, -\cos \theta^*) \end{aligned}$$

from which one can derive

$$\hat{t} = -\frac{\hat{s}}{2}(1 - \cos(\theta^*)) \quad \hat{u} = -\frac{\hat{s}}{2}(1 + \cos(\theta^*)).$$

Next, write the parton four-vectors in the hadron-hadron frame as

$$p_1 = \frac{\sqrt{s}}{2} x_a (1, 0, 0, 1)$$

$$p_2 = \frac{\sqrt{s}}{2} x_b (1, 0, 0, -1)$$

$$p_3 = p_T (\cosh y_3, 1, 0, \sinh y_3)$$

$$p_4 = p_T (\cosh y_4, -1, 0, \sinh y_4)$$

which can be used to derive

$$\begin{aligned}\hat{t} &= -\sqrt{s}x_\alpha p_T e^{-y_3} \\ \hat{u} &= -\sqrt{s}x_\alpha p_T e^{-y_4}.\end{aligned}$$

From these two sets of expressions one can obtain

$$\frac{\hat{t}}{\hat{u}} = e^{-(y_3 - y_4)} = \frac{1 - \cos \theta^*}{1 + \cos \theta^*}.$$

It then follows that

$$\cos \theta^* = \tanh \frac{y_3 - y_4}{2}.$$

8. Some comments on the asymptotic solution of the evolution equations for parton distributions in a photon

- Rewrite the evolution equations by taking moments of both sides using the following definitions:

$$M_q^n = \int_0^1 dx x^{n-1} G_{q/\gamma}(x)$$

$$M_g^n = \int_0^1 dx x^{n-1} G_{g/\gamma}(x)$$

$$A_{ij}^n = \frac{1}{2\pi b} \int_0^1 dx x^{n-1} P_{ij}(x)$$

$$a^n = \frac{\alpha}{2\pi} \int_0^1 dx x^{n-1} P_{q\gamma}$$

$$\alpha_s(t) = \frac{1}{bt}$$

where $t = \ln(Q^2/\Lambda^2)$.

- The evolution equations can now be written as

$$\begin{aligned}\frac{dM_q^n}{dt} &= e_q^2 a^n + \frac{1}{t} [A_{qq}^n M_q^n + A_{qg}^n M_g^n] \\ \frac{dM_g^n}{dt} &= \frac{1}{t} \left[\sum_q A_{gq}^n M_q^n + A_{gg}^n M_g^n \right]\end{aligned}$$

- If each of the moments is proportional to t , the t dependence drops out of the equations and they may be solved algebraically

- The asymptotic solution is

$$\begin{aligned}
 M_q^n &= a^n \left(\frac{e_q^2 - 5/18}{1 - A_{qq}^n} + \frac{5}{18} \frac{1 - A_{gg}^n}{F^n} \right) t \\
 M_g^n &= \frac{5f}{9} a^n \frac{A_{gg}^n}{F^n} t \\
 F^n &= 1 - A_{qq}^n - A_{gg}^n + A_{qq}^n A_{gg}^n - 2f A_{qq}^n A_{gq}^n
 \end{aligned}$$

where f is the number of flavors

- Note how the moments are each proportional to t
- Compare to the case where $P_{q\gamma} = 0$ where the moments are of the form

$$M^n(t_0) \left(\frac{t}{t_0} \right)^{A^n}$$

- Note that one can add any solution of the homogeneous evolution equations to this asymptotic solution